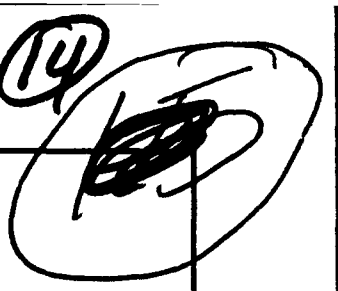

COLLEGE PARK CAMPUS

A-POSTERIORI ESTIMATION AND ADAPTIVE CONTROL OF THE POLLUTION-ERROR IN THE *h*-VERSION OF THE FINITE ELEMENT METHOD

by

I. Babuška
T. Strouboulis
C. S. Upadhyay
S. K. Gangaraj

Technical Note BN-1175

and

CMC Report No. 94-06
Texas Engineering Experiment Station
The Texas A&M University System

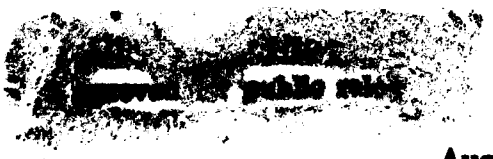

August 1994

INSTITUTE FOR PHYSICAL SCIENCE AND TECHNOLOGY

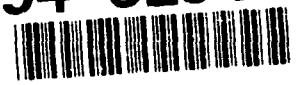

SECURITY CLASSIFICATION OF THIS PAGE (When Data Entered)

REPORT DOCUMENTATION PAGE		READ INSTRUCTIONS BEFORE COMPLETING FORM
1. REPORT NUMBER [1]Technical Note BN-1175	2. GOVT ACCESSION NO.	3. RECIPIENT'S CATALOG NUMBER
4. TITLE (and Subtitle) A-Posteriori Estimation and Adaptive Control of the Pollution-Error ih the h-Version of the Finite Element Method		5. TYPE OF REPORT & PERIOD COVERED Final Life of Contract 6. PERFORMING ORG. REPORT NUMBER
7. AUTHOR(s) I. Babuska[1] - T. Strouboulis[2] - C. S. Upadhyay[2] S. K. Gangaraj[2]		8. CONTRACT OR GRANT NUMBER(s) [1]N00014-90-J-1030 (ONR) & CCR-88-20279 (NSF) [2]See Page 1
9. PERFORMING ORGANIZATION NAME AND ADDRESS [1]Institute for Physical Science and Technology University of Maryland College Park, MD 20742-2431		10. PROGRAM ELEMENT, PROJECT, TASK AREA & WORK UNIT NUMBERS
11. CONTROLLING OFFICE NAME AND ADDRESS Department of the Navy Office of Naval Research Arlington, VA 22217		12. REPORT DATE August 1994 13. NUMBER OF PAGES 38 + Figs. 1 - 9b
14. MONITORING AGENCY NAME & ADDRESS(if different from Controlling Office)		15. SECURITY CLASS. (of this report) 15a. DECLASSIFICATION/DOWNGRADING SCHEDULE

16. DISTRIBUTION STATEMENT (of this Report)

Approved for public release: distribution unlimited

17. DISTRIBUTION STATEMENT (of the abstract entered in Block 20, if different from Report)

18. SUPPLEMENTARY NOTES

19. KEY WORDS (Continue on reverse side if necessary and identify by block number)

20. ABSTRACT (Continue on reverse side if necessary and identify by block number)

In [1] (resp. [2]) we studied the pollution-error in the h-version of the finite element method and its effect on the quality of the local error indicators (resp. the quality of the derivatives recovered by local postprocessing) in the interior of the mesh. Here we show that it is possible to construct a-posteriori estimates of the pollution-error in a patch of elements by employing the local error indicators over the entire mesh. We also give an adaptive algorithm for the local control of the pollution-error in a patch of elements of interest.

DD FORM 1 JAN 73 1473 EDITION OF 1 NOV 65 IS OBSOLETE

S/N 0102-LF-014-6601

SECURITY CLASSIFICATION OF THIS PAGE (When Data Entered)

A-Posteriori Estimation and Adaptive Control of the Pollution-Error in the *h*-Version of the Finite Element Method

I. Babuška*
Institute for Physical Science and Technology and Department of Mathematics,
University of Maryland, College Park, MD 20742, U.S.A.

T. Strouboulis†, C.S. Upadhyay† and S.K. Gangaraj†
Department of Aerospace Engineering, Texas A&M University,
College Station, TX 77843, U.S.A.

August 1994

*The work of this author was supported by the U.S. Office of Naval Research under Contract N00014-90-J-1030 and by the National Science Foundation under Grant CCR-88-20279.

†The work of these authors was supported by the U.S. Army Research Office under Grant DAAL03-G-028, by the National Science Foundation under Grant MSS-9025110 and by the Texas Advanced Research Program under Grant TARP-71071.

Abstract

In [1] (resp. [2]) we studied the pollution-error in the h-version of the finite element method and its effect on the quality of the local error indicators (resp. the quality of the derivatives recovered by local postprocessing) in the interior of the mesh. Here we show that it is possible to construct a-posteriori estimates of the pollution-error in a patch of elements by employing the local error indicators over the entire mesh. We also give an adaptive algorithm for the local control of the pollution-error in a patch of elements of interest.

1 Introduction

Let $\Omega \subseteq \mathbf{R}^2$ denote a polygonal domain with boundary $\partial\Omega = \Gamma = \bigcup_{i=1}^{M} \bar{\Gamma}_i$, where Γ_i, $i = 1, \ldots, M$ are the open straight edges connecting the endpoints A_i and A_{i+1} ($A_1 = A_{M+1}$) (see Fig. 1). We will denote the internal angles at the vertices by $\varphi_1, \ldots, \varphi_M$ ($0 < \varphi_i \leq 2\pi$; if $\varphi_i = 2\pi$ we have a *slit-domain* and in this case we have to understand the boundary in the obviously modified sense). Further, let $\Gamma = \bar{\Gamma}_D \cup \Gamma_N$, $\bar{\Gamma}_D \cap \Gamma_N = \emptyset$ where Γ_D is the *Dirichlet-* and Γ_N is the *Neumann*-boundary. We will consider the mixed boundary-value problem for the Laplacian:

$$-\Delta u := -\nabla \cdot \nabla u = 0 \qquad \text{in } \Omega \tag{1a}$$

$$u = 0 \qquad \text{on } \Gamma_D \tag{1b}$$

$$\frac{\partial u}{\partial n} := \nabla u \cdot \boldsymbol{n} = g \qquad \text{on } \Gamma_N \tag{1c}$$

Here u is the exact solution; $\boldsymbol{n}$ denotes the exterior unit-normal on Γ_N; $g \in L^2(\Gamma_N)$ and is smooth in each Γ_j, $j = 1, \ldots, M$.

The variational formulation of the model problem (1) is:

$$\text{Find } u \in H^1_{\Gamma_D} := \left\{ u \in H^1(\Omega) \;\middle|\; u = 0 \text{ on } \Gamma_D \right\} \text{ such that}$$

$$B_\Omega(u, v) := \int_\Omega \nabla u \cdot \nabla v = \int_{\Gamma_N} gv \qquad \forall\, v \in H^1_{\Gamma_D} \tag{2}$$

If $\Gamma_D = \emptyset$ it is assumed that g satisfies the consistency condition $\int_\Gamma g = 0$; in this case the solution u is determined uniquely up to an arbitrary constant.

For the finite element method we partition the domain Ω into triangular or square elements with straight edges τ defined by the mesh T_h and let

$$S_h^p(\Omega) := \left\{ v_h \in H^1_{\Gamma_D} \;\middle|\; v_h|_\tau \in S_h^p(\tau) \qquad \forall\, \tau \in T_h \right\} \tag{3}$$

Here $S_h^p(\tau)$ denotes the *finite-element space* over τ and p is the degree of the elements. For the meshes of triangles $S_h^p(\tau) \equiv \mathcal{P}_p(\tau)$, while for the meshes of squares $S_h^p(\tau)$ denotes the *tensor-product polynomial space of degree p*

$$S_h^p(\tau) := \left\{ P \;\middle|\; P(x_1, x_2) = \sum_{\substack{i,j \\ 0 \leq i,j \leq p}} \alpha_{i,j}\, x_1^i\, x_2^j \right\} \tag{4}$$

The finite element approximation of the solution of (1) satisfies:

Find $u_h \in S^p_{h,\Gamma_D} := S^p_h(\Omega) \bigcap H^1_{\Gamma_D}$ such that

$$B_\Omega(u_h, v_h) = \int_{\Gamma_N} g\, v_h \qquad \forall\ v_h \in S^p_{h,\Gamma_D} \tag{5}$$

There exists a large literature devoted to the a-posteriori estimation of the error of the finite element solution $e_h := u - u_h$, and to the recovery of the data of interest (e.g. derivatives, stresses, etc.). For a complete discussion and references to the vast literature see [3]-[8] for the problem of a-posteriori error estimation and [9]-[13] for the problem of the recovery. All of these procedures have *local character* i.e. the computed data in the element or patch of elements depend on the finite element solution and the input-data *only in the neighborhood of the element or patch* under consideration. In [6]-[8] and the theory presented there we underlined the assumption that the mesh outside the region of interest has to be appropriate so that there is no significant pollution, which *cannot be detected by any local analysis*. We have shown in detail the effect of the pollution on the a-posteriori error estimation and recovery in [1] and [2], respectively.

In [1] and [2] we have seen that *the pollution-effect is negligible for meshes which are constructed adaptively with respect to the energy error-measure in the entire domain* (we will call such a mesh a *fully-adaptive mesh*). Nevertheless, very often in engineering computations, the mesh employed is very different from a fully-adaptive mesh because of limited computer resources. *It is often assumed that the computed data are reliable* (if this is indicated by the local error estimates or the difference between the recovered data and the data computed-directly from the finite element solution) *without paying attention to the refinement of the mesh outside the region of interest*, as it is done, for example, in the global-local approach [14]-[16]. This assumption can be correct or false, as has been shown in the results given in [1] and [2] (see also [17]). From these results it is clear that *there is urgent need* for the a-posteriori control of the pollution. This control *cannot be local*, has to be cheap and accurate and will be addressed in the present paper. We will assume that we have at our disposition error indicators which are very robust *modulo the pollution* (i.e. the element effectivity indices are close to one if there is no pollution). We have shown (see [6]-[8]) several examples of robust indicators in the interior of the mesh. The analysis of the various error indicators for the elements at the boundary and especially for the unsmooth solutions (in the neighborhood of the singular points) will be done in forthcoming papers. In the present paper we mention only a few illustrative examples related to the standard estimators.

2 Local error indicators

Below we describe two types of local error indicators which will be used in the numerical examples for the construction of a-posteriori estimates of the pollution.

2.1 Error indicators based on patch-recovery

Let ω_X denote the patch of elements connected to vertex X. For each patch ω_X we recover the *smoothened-gradient* $\tilde{\boldsymbol{q}}^X$, by solving the following least-squares problem:

$$||\boldsymbol{\nabla} u_h - \tilde{\boldsymbol{q}}^X||_{L^2(\omega_X),\{y_\ell\}_{\ell=1}^{nsp}} = \inf_{q^X \in (\mathcal{P}_p(\omega_X))^2} ||\boldsymbol{\nabla} u_h - \boldsymbol{q}^X||_{L^2(\omega_X),\{y_\ell\}_{\ell=1}^{nsp}} \tag{6}$$

where $\{\boldsymbol{y}_\ell\}_{\ell=1}^{nsp}$ denotes a set of *sampling points* in ω_X (given in [18-20]) and

$$||\boldsymbol{q}||^2_{L^2(\omega_X),\{y_\ell\}_{\ell=1}^{nsp}} := \sum_{m=1}^{nsp} \left[\sum_{i=1}^{2} \left(q_i(\boldsymbol{y}_m) \right)^2 \right] \tag{7}$$

A continuous piecewise polynomial *recovered gradient* $\boldsymbol{q}^{ZZ}$ is obtained over the mesh by combining the smoothened-gradient $\tilde{\boldsymbol{q}}^X$ from the patches which correspond to the vertices of the element (see [18-20] for the details). In the construction of $\boldsymbol{q}^{ZZ}$ we employ only patches ω_X for vertices X in the interior of the domain. The values of $\boldsymbol{q}^{ZZ}$ at the boundary are obtained using extrapolation from the interior patches. The element error indicators are given by:

$$\eta_\tau^{ZZ} := ||\boldsymbol{q}^{ZZ} - \boldsymbol{\nabla} u_h||_{L^2(\tau)} \tag{8}$$

In the numerical examples we will call this estimator the ZZ (Zienkiewicz-Zhu)-estimator.

2.2 Error indicators based on element-residual problems

Let ε be an edge and J_ε denote the *jump of the normal derivative of* u_h *on* ε, defined by:

$$J_\varepsilon := \begin{cases} \left(\boldsymbol{\nabla} u_h \big|_{\tau_{in}} - \boldsymbol{\nabla} u_h \big|_{\tau_{out}} \right) \cdot \boldsymbol{n}, & \varepsilon \not\subseteq \partial\Omega \\ 2\left(g - \boldsymbol{\nabla} u_h \big|_{\tau_{out}} \right) \cdot \boldsymbol{n}, & \varepsilon \subseteq \Gamma_N \\ 0, & \varepsilon \subseteq \Gamma_D \end{cases} \tag{9}$$

Here $\boldsymbol{n}$, τ_{in} and τ_{out} denote the unit-normal and the elements associated with the edge ε, as shown in Fig. 2. We will denote by $r_\tau := \Delta u_h \big|_\tau$ the *interior residual* for element τ and let $\mathcal{F}_\tau : H^1_{\Gamma_D} \to \mathbf{R}$ be the *residual functional* given by

$$\mathcal{F}_\tau(v) := \int_\tau v r_\tau + \frac{1}{2} \sum_{\epsilon \subseteq \partial\tau} \int_\epsilon v J_\epsilon, \qquad v \in H^1_{\Gamma_D} \tag{10}$$

The error e_h satisfies the *residual-equation*:

Find $e_h \in H^1_{\Gamma_D}$ such that

$$B_\Omega(e_h, v) = \sum_{\tau \in T_h} \mathcal{F}_\tau(v) \qquad \forall\ v \in H^1_{\Gamma_D} \tag{11}$$

Let us assume that the element-residuals have been modified in the following way (for the construction see the Appendix):

$$\mathcal{F}^{EQ}_\tau(v) := \mathcal{F}_\tau(v) + \sum_{\varepsilon \subseteq \partial\tau \cap E_{int}} \int_\varepsilon v\theta^\varepsilon_\tau \tag{12}$$

such that

$$\mathcal{F}^{EQ}_\tau(v) = 0 \qquad \forall\ v \in S^p_h(\tau) \tag{13}$$

Here θ^ε_τ is the *correction* for the edge ε and the element τ and E_{int} denotes the set of interior edges. For any interior edge ε the correction θ^ε_τ is constructed such that $\theta^\varepsilon_{\tau_{in}} = -\theta^\varepsilon_{\tau_{out}}$. We then have

$$\sum_{\tau \in T_h} \mathcal{F}_\tau(v) = \sum_{\tau \in T_h} \mathcal{F}^{EQ}_\tau(v) \tag{14}$$

Let us introduce the local problems:

For each element $\tau \in T_h$ find $\hat{e}_\tau \in H^1(\tau)$ such that

$$B_\tau(\hat{e}_\tau, v) = \mathcal{F}^{EQ}_\tau(v) \qquad \forall\ v \in H^1(\tau) \tag{15}$$

Note that $\hat{e}_\tau$ exists and is unique up to a constant since $\mathcal{F}^{EQ}_\tau(1) = 0$. (If $\partial\tau \bigcap \Gamma_D \neq \emptyset$ we let $\hat{e}_\tau|_\varepsilon = 0$ for edges $\varepsilon \in \partial\tau \bigcap \Gamma_D$ and, in this case, the solution is unique.) Let us denote by $|||v|||_S := \sqrt{B_S(v,v)}$ the energy norm over any $S \subseteq \Omega$. We then have

$$|||e_h|||_\Omega = \sup_{v \in H^1_{\Gamma_D}} \frac{\sum_{\tau \in T_h} B_\tau(e_h, v)}{|||v|||_\Omega} = \sup_{v \in H^1_{\Gamma_D}} \frac{\sum_{\tau \in T_h} \mathcal{F}_\tau(v)}{|||v|||_\Omega} = \sup_{v \in H^1_{\Gamma_D}} \frac{\sum_{\tau \in T_h} \mathcal{F}^{EQ}_\tau(v)}{|||v|||_\Omega} \tag{16a}$$

and hence

$$|||e_h|||_\Omega = \sup_{v \in H^1_{\Gamma_D}} \frac{\sum_{\tau \in T_h} B_\tau(\hat{e}_\tau, v)}{|||v|||} \leq \sqrt{\sum_{\tau \in T_h} |||\hat{e}_\tau|||^2_\tau} \tag{16b}$$

Thus *an upper-estimator for the global energy-norm of the error is obtained provided that the local problems are solved exactly.* We will denote this estimator by ERp.

In the implementations we employed approximate solutions of the local problems which are computed as follows:

Find $\hat{e}_\tau^{(p+k)} \in \mathcal{P}^{p+k}(\tau)$ such that

$$B_\tau(\hat{e}_\tau^{(p+k)}, v) = \mathcal{F}_\tau^{EQ}(v) \qquad \forall\ v \in \mathcal{P}^{p+k}(\tau) \tag{17}$$

with the corresponding element error indicators

$$\hat{\eta}_\tau^{(p+k)} := |||\hat{e}_\tau^{(p+k)}|||_\tau \tag{18}$$

In the numerical examples we will denote the estimator defined by (17) and (18) as ERpP$p+k$ (element-residual with p-order equilibration and $(p+k)$-degree polynomial space). For further details about element-residual estimators see [8], [21-29] and the references therein.

Remark 2.1: By letting $k \longrightarrow \infty$ in (17) we recover the exact solution $\hat{e}_\tau$ of the local problem (15). In most cases, by letting $k = 3$ we obtain element error indicators which are practically the same as the indicators corresponding to the exact solutions of the local problems.

We also considered the following variation of the local residual problem:

Find $\tilde{e}_\tau^{(p+1)} \in M_p^{p+1}(\tau)$ such that

$$B_\tau(\tilde{e}_\tau^{(p+1)}, v) = \mathcal{F}_\tau^{EQ}(v) \qquad \forall\ v \in M_p^{p+1}(\tau) \tag{19}$$

Here $M_p^{p+1}(\tau)$ is the *bubble-space* of degree $(p+1)$ (see [28]-[29]). In the computations we employed the hierarchical element families given in [30] and let $M_p^{p+1}(\tau)$ be the span of the edge shape-functions of degree $(p+1)$ only (i.e. three (resp. four) edge shape-functions for a triangular (resp. square) element) together with all interior shape-functions in $S_h^{p+1}(\tau)$. We will call the estimator based on (19) the ERpB-estimator (element-residual with p-order equilibration and with $(p+1)$-degree bubble space). (For a detailed study of the element-residual estimators in the interior of the mesh see [6-8].)

We also considered the following *patch-residual estimator*: Let τ be the element of interest, ω_h be a patch of elements which includes τ and a few mesh-layers around it and consider the local problem:

Find $e_{\omega_h}^{(p+k)} \in S_{h,0}^p(\omega_h)$ such that

$$\sum_{\tau \subseteq \omega_h} B_\tau(e_{\omega_h}^{(p+k)}, v) = \sum_{\tau \subseteq \omega_h} \mathcal{F}_\tau^{EQ}(v) \qquad \forall\ v \in S_{h,0}^p(\omega_h) \tag{20}$$

Here we let

$$S^p_{h,0}(\omega_h) := \left\{ v \in C^0(\omega_h) \;\middle|\; v|_\tau \in S^p_h(\tau), \quad v = 0 \quad \text{on} \quad \partial\omega_h \cap \Gamma_D \right\} \tag{21}$$

The error-indicator in the element τ is computed by

$$\eta^{(p+k)}_\tau = |||e^{(p+k)}_{\omega_h}|_\tau|||_\tau \tag{22}$$

We will use the notation PRpP$p+k$ to refer to the patch-residual problem with equilibration of order p and $(p+k)$-degree polynomial space. Below we will consider patches which consist of a few mesh-layers of elements around the singular point.

2.3 The quality of the error-indicators in the neighborhood of the singular points

We now give sample results on the quality of the error indicators in the neighborhood of singular points for uniform meshes of triangles and squares; we will present a more systematic study in a forthcoming paper.

Let us consider the problem (1) in the L-shaped domain $(-1,1)^2 - [0,1]\times[0,-1]$ (resp. the slit domain $(-1,1)^2 - [0,1]$) and assume that the boundary-conditions are such that (for a complete study of the properties of solutions in polygonal domains, see [31]-[34]) $u(r,\vartheta) = r^\alpha \psi(\alpha\vartheta)$ where (r,ϑ) are polar coordinates with $r = 0$ at the singular point. We employed homogeneous boundary-conditions on the edges of the domain emanating from the singular-point at (0,0) such that $\psi(\alpha\vartheta) = \sin(\alpha\vartheta)$ (resp. $\psi(\alpha\vartheta) = \cos(\alpha\vartheta)$) for homogeneous Dirichlet or mixed (resp. homogeneous Neumann) boundary conditions, and Neumann boundary-conditions computed from the exact solution in the rest of the boundary. We employed the values $\alpha = \frac{1}{3}$ and $\frac{2}{3}$ in the case of the L-shaped domain $\left(\text{resp. } \alpha = \frac{1}{4} \text{ and } \alpha = \frac{1}{2} \text{ for the slit-domain}\right)$. We computed the finite element solution using the uniform-meshes of triangles with $h = \frac{1}{16}$ shown in Fig. 4a, for the L-shaped domain, and in Fig. 5a for the slit-domain.

In Tables 1a, 1b (resp. Tables 1c, 1d) we give the effectivity indices for the various estimators in the neighborhood of the singular point for linear (resp. quadratic) triangles. The effectivity indices are given for the elements near the singularity shown in Figs. 4b, 5b. In Tables 1a-1d we included the estimators ERpP$p+1$, ERpB, ZZ and PRpP$p+3$ (for the patch-residual estimator we employed two mesh-layers around the singular point to define the patch). In Table 2 we give the effectivity indices for the estimators ERpP$p+k$ for $k = 1, 2, 3, 4$, PRpP$p+3$ and ZZ for the L-shaped domain with $\alpha = \frac{1}{3}$ where the finite element solution was

computed using the uniform mesh of bilinear-squares shown in Fig. 6a $\left(p = 1,\ h = \frac{1}{32}\right)$. The effectivity indices are reported for the elements in the neighborhood of the singular point shown in Fig. 6b. Note that for the meshes of squares we employed three mesh-layers around the singular-point as the patch for the estimator PRpP$p+3$.

We see that the error in the layer of elements adjacent to the singularity can be relatively large (e.g. more than 50% of the error in the entire mesh). The elements where the energy of the error is more than 10% of the global energy of the error will be called *key elements*. The large spread of the effectivity indices in the key elements is in contrast to the robustness of the estimators for smooth solutions and interior elements that we reported in [6]-[8].

As we said above the quality of the pollution estimates depends on the quality of the estimator. Hence we should also consider another estimator which is very accurate in the key elements. Such an estimator can be obtained by assuming the asymptotic expansion

$$u(r,\vartheta) = \sum_{i=1}^{3} C_i\, r^{\alpha_i} \sin(\alpha_i \vartheta) \tag{23}$$

$\left(\text{or } u(r,\vartheta) = \sum C_i\, r^{\alpha_i} \cos(\alpha_i \vartheta) \text{ depending on the boundary-conditions}\right)$ and by extracting the coefficients C_i from the finite element solution by employing the contour-integral method given in [30]. For example for the case of the strongest singularity $\alpha = \frac{1}{4}$, the mesh shown in Fig. 5a and the elements shown in Fig. 5b the effectivity indices, obtained by the extraction method, are,

$$\left.\begin{array}{lll} \kappa_{\tau_1} = 0.91, & \kappa_{\tau_2} = 0.91, & \kappa_{\tau_3} = 0.93 \\ \kappa_{\tau_4} = 0.95, & \kappa_{\tau_5} = 0.97, & \kappa_{\tau_6} = 0.99 \end{array}\right\} \tag{24a}$$

for linear triangles ($p = 1$) and

$$\left.\begin{array}{lll} \kappa_{\tau_1} = 0.91, & \kappa_{\tau_2} = 0.92, & \kappa_{\tau_3} = 0.94 \\ \kappa_{\tau_4} = 0.97, & \kappa_{\tau_5} = 0.99, & \kappa_{\tau_6} = 1.00 \end{array}\right\} \tag{24b}$$

for quadratic triangles ($p = 2$). Comparing the above effectivity indices with the effectivity indices reported in Tables 1b, 1d we see significant improvement in the quality of the estimator in the key-elements.

Remark 2.1. In the examples below we know the exact solution and we could get the exact error indicators. We employ the extraction method as a general approach

for the error computation. We will discuss the construction of error-indicators in the neighborhood of singular points in a forthcoming paper.

3 A posteriori estimate of the pollution error

In Section 2 we introduced various error estimates. We will now consider the estimator ERp.

Let ω_h be a patch of elements (possibly consisting of one element) and let $\tilde{\omega}_h$ denote a patch which consists of ω_h and a few mesh-layers around it (e.g. Fig. 3). From (11)-(14) we get

$$B_\Omega(e_h, v) = \sum_{\tau \in T_h} \mathcal{F}_\tau^{EQ}(v) \qquad \forall\ v \in H^1_{\Gamma_D} \tag{25}$$

Let $V_j^{\tilde{\omega}_h} \in H^1_{\Gamma_D}$ for $j = 1, 2$, be defined by

$$B_\Omega(V_1^{\tilde{\omega}_h}, v) = \sum_{\substack{\tau \in T_h \\ \tau \subseteq \tilde{\omega}_h}} \mathcal{F}_\tau^{EQ}(v) \qquad \forall\ v \in H^1_{\Gamma_D} \tag{26}$$

$$B_\Omega(V_2^{\tilde{\omega}_h}, v) = \sum_{\substack{\tau \in T_h \\ \tau \not\subseteq \tilde{\omega}_h}} \mathcal{F}_\tau^{EQ}(v) \qquad \forall\ v \in H^1_{\Gamma_D} \tag{27}$$

Obviously

$$V_1^{\tilde{\omega}_h} + V_2^{\tilde{\omega}_h} = e_h \tag{28}$$

In [1] we showed that, in general, we have

$$\mathcal{E}_{\omega_h} \approx |||V_1^{\tilde{\omega}_h}|||_{\omega_h} \qquad \text{as} \quad h \longrightarrow 0 \tag{29}$$

The symbol $\approx$ means that there exist constants $C_L^{\tilde{\omega}_h}$, $C_U^{\tilde{\omega}_h}$, which depend on the geometry of the mesh in $\tilde{\omega}_h$, but not on the mesh-size h, such that

$$C_L^{\tilde{\omega}_h} \mathcal{E}_{\omega_h} \leq |||V_1^{\tilde{\omega}_h}|||_{\omega_h} \leq C_U^{\tilde{\omega}_h} \mathcal{E}_{\omega_h} \tag{30}$$

In [6]-[8] we computed the values of $C_L^{\tilde{\omega}_h}$, $C_U^{\tilde{\omega}_h}$ for several estimators and a variety of meshes and identified several *robust estimators* (e.g. estimators with $C_L^{\tilde{\omega}_h}$ and $C_U^{\tilde{\omega}_h}$ close to one for the types of meshes which occur in practical computations) for mesh-cells ω_h in the interior of the mesh. Here, as usual, we let $\mathcal{E}_{\omega_h} := \Big(\sum_{\tau \in \omega_h} \eta_\tau^2\Big)^{\frac{1}{2}}$ with η_τ being the element error-indicator corresponding to the particular estimator (e.g. ERp). From (28)-(30) (and the results in [1]) we see that $|||V_2^{\tilde{\omega}_h}|||_{\omega_h}$ is the

measure of the pollution and that the estimate of the pollution is equivalent with the estimate of $|||V_2^{\tilde{\omega}_h}|||_{\omega_h}$. We also note that $V_2^{\tilde{\omega}_h}$ is harmonic in ω_h.

Let $G_i^{(\bar{x})}$, $\bar{x} \in \Omega$, be the function satisfying

$$-\Delta G_i^{(\bar{x})} = -\frac{\partial \delta}{\partial x_i}(\bar{x}) \qquad \text{in} \quad \Omega \tag{31a}$$

$$G_i^{(\bar{x})} = 0 \qquad \text{on} \quad \Gamma_D \tag{31b}$$

$$\frac{\partial}{\partial n} G_i^{(\bar{x})} = 0 \qquad \text{on} \quad \Gamma_N \tag{31c}$$

Here $i = 1$ or 2 and $\frac{\partial \delta}{\partial x_i}(\bar{x})$ denotes the x_i-derivative of Dirac's delta centered at $\bar{x}$. Eq. (31a) is understood in the sense of the theory of distributions. Obviously $G_i^{(\bar{x})} \notin H^1_{\Gamma_D}$. By the standard arguments we see that

$$\frac{\partial V_2^{\tilde{\omega}_h}}{\partial x_i}(\bar{x}) = \sum_{\substack{\tau \in T_h \\ \tau \not\subset \tilde{\omega}_h}} \mathcal{F}_\tau^{EQ}(G_i^{(\bar{x})}) \tag{32}$$

Let us now replace the function $G_i^{(\bar{x})}$ by the difference

$$\tilde{G}_i^{(\bar{x})}(\boldsymbol{x}) := \frac{1}{h}\Big(G^{(\bar{x}+h\boldsymbol{n}_i)}(\boldsymbol{x}) - G^{(\bar{x})}(\boldsymbol{x})\Big) \tag{33}$$

where $\boldsymbol{n}_i$ denotes the unit-vector in the i-th coordinate direction and $G^{(\bar{x})}$ is the (classical) Green's function. Then for any $\boldsymbol{x} \in \Omega - \tilde{\omega}_h$ we have

$$\Big|\tilde{G}_i^{(\bar{x})}(\boldsymbol{x}) - G_i^{(\bar{x})}(\boldsymbol{x})\Big| \leq Ch \tag{34}$$

We note that we can replace $G_i^{(\bar{x})}$ by another combination of Green's functions so that the error will be of order h^s ($s > 0$, arbitrary) instead of order h as in (34). Using (13) and (32) we get

$$\frac{\partial V_2^{\tilde{\omega}_h}}{\partial x_i}(\bar{x}) = \sum_{\substack{\tau \in T_h \\ \tau \not\subset \tilde{\omega}_h}} \mathcal{F}_\tau^{EQ}(G_i^{(\bar{x})} - w_\tau) \tag{35}$$

where w_τ is the best-approximation of $G_i^{(\bar{x})}$ on τ from $S_h^p(\tau)$ in the energy-norm. By employing the definition of $\hat{e}_\tau$ (see (15)) we see that

$$\frac{\partial V_2^{\tilde{\omega}_h}}{\partial x_i}(\bar{x}) = \sum_{\substack{\tau \in T_h \\ \tau \not\subset \tilde{\omega}_h}} B_\tau(\hat{e}_\tau, G_i^{(\bar{x})} - w_\tau) \tag{36}$$

Hence

$$\Big|\frac{\partial V_2^{\tilde{\omega}_h}}{\partial x_i}(\bar{\boldsymbol{x}})\Big| \leq \sum_{\substack{\tau \in T_h \\ \tau \not\subset \tilde{\omega}_h}} |||\hat{e}_\tau|||_\tau |||G_i^{(\bar{x})} - w_\tau|||_\tau \tag{37}$$

Replace now $G_i^{(\bar{x})}$ by $\tilde{G}_i^{(\bar{x})}$ and w_τ by $\tilde{w}_\tau$ $\Big(\tilde{w}_\tau$ is the best-approximation of $\tilde{G}_i^{(\bar{x})}$ on $\tau\Big)$ to obtain

$$\Big|\frac{\partial V_2^{\tilde{\omega}_h}}{\partial x_i}(\bar{\boldsymbol{x}})\Big| \leq \sum_{\substack{\tau \in T_h \\ \tau \not\subset \tilde{\omega}_h}} \eta_\tau(u_h) |||\tilde{G}_i^{(\bar{x})} - \tilde{w}_\tau|||_\tau (1 + Ch) \tag{38}$$

where $\eta_\tau(u_h)$ is the ERp-indicator computed from u_h. Because $\tilde{w}_\tau$ is the best-approximation on τ of the function $\tilde{G}_i^{(\bar{x})}$ we get

$$|||\tilde{G}_i^{(\bar{x})} - \tilde{w}_\tau|||_\tau \leq \eta_\tau(\tilde{G}_{i,h}^{(\bar{x})}) \tag{39}$$

and using (38) we obtain

$$\Big|\frac{\partial V_2^{\tilde{\omega}_h}}{\partial x_i}(\bar{\boldsymbol{x}})\Big| \leq \Big(\sum_{\substack{\tau \in T_h \\ \tau \not\subset \tilde{\omega}_h}} \eta_\tau(u_h)\ \eta_\tau(\tilde{G}_{i,h}^{(\bar{x})})\Big)(1 + Ch) \tag{40}$$

Here we are assuming that $\bar{\boldsymbol{x}}$ is a nodal point of the mesh and that $\eta_\tau(\tilde{G}_{i,h}^{(\bar{x})})$ is the ERp-indicator computed from the finite element solution $\tilde{G}_{i,h}^{(\bar{x})} \in S^p_{h,\Gamma_D}$ which satisfies

$$B_\Omega(\tilde{G}_{i,h}^{(\bar{x})}, v) = \frac{1}{h}\Big(v(\bar{\boldsymbol{x}} + \boldsymbol{n}_i h) - v(\bar{\boldsymbol{x}})\Big) \qquad \forall\ v \in S^p_{h,\Gamma_D} \tag{41}$$

We assume that $\bar{\boldsymbol{x}} + \boldsymbol{n}_i h$ is also a nodal point of the mesh (this can be always achieved with obvious modifications of the approximation of $G_i^{(\bar{x})}$).

We note that $\tilde{G}_{i,h}^{(\bar{x})}$ approximates well the function $\tilde{G}_i^{(\bar{x})}$ on $\Omega - \tilde{\omega}_h$, although $G_i^{(\bar{x})}$ does not belong to $H^1_{\Gamma_D}$. Note that $G_i^{(\bar{x})}$ has singular behavior at the corner-points. For further details see [35]-[36]. Note also that $\tilde{G}_{i,h}^{(\bar{x})}$ $\Big($and hence the corresponding error indicators $\eta_\tau(\tilde{G}_i^{(\bar{x})})\Big)$ is cheap to compute because it requires only the solution of the system of discrete equations for an additional right-hand side.

We employ the indicator $\eta_\tau(\tilde{G}_{i,h}^{(\bar{x})})$ only as an estimate of the error in the best-approximation on the left hand side of (39) and hence the possible pollution does not play any role. Also, from the construction of $V_2^{\tilde{\omega}_h}$, we see that it relates only to the residuals (which are local) and hence the absence of the pollution-term from $\eta_\tau(u_h)$ does not influence the accuracy of the estimate (40). Hence the only

requirement for the reliability of (40) is the accuracy of the indicators *modulo the pollution*. Further, since $V_2^{\tilde{\omega}_h}$ is smooth in ω_h we can approximate $|||V_2^{\tilde{\omega}_h}|||_{\omega_h}$ assuming that $\nabla V_2^{\tilde{\omega}_h}$ is constant in ω_h by letting

$$|||V_2^{\tilde{\omega}_h}|||_{\omega_h} \cong \sqrt{|\omega_h|}\sqrt{\Big(\frac{\partial V_2^{\tilde{\omega}_h}}{\partial x_1}(\bar{\boldsymbol{x}})\Big)^2 + \Big(\frac{\partial V_2^{\tilde{\omega}_h}}{\partial x_2}(\bar{\boldsymbol{x}})\Big)^2} \tag{42}$$

with $\bar{\boldsymbol{x}} \in \omega_h$.

Remark 3.1. Although we mentioned the pollution error in connection with the error estimate in ω_h, the same idea can also be used to estimate the effect of the pollution on the error in recovered quantities.

In summary the a-posteriori estimate of $\Big|\frac{\partial V_2^{\tilde{\omega}_h}}{\partial x_i}(\bar{\boldsymbol{x}})\Big|$ is constructed as follows:

We compute the indicators $\eta_\tau(u_h)$, $\eta_\tau(\tilde{G}_{i,h}^{(\bar{x})})$ and define

$$\mathcal{M}_i^{(1)}(\bar{\boldsymbol{x}}) = \sum_{\substack{\tau \in T_h \\ \tau \subset \tilde{\omega}_h}} \Big| B_\tau\Big(\hat{e}_\tau(u_h), \hat{e}_\tau(\tilde{G}_{i,h}^{(\bar{x})})\Big)\Big| \tag{43}$$

where $\hat{e}_\tau(u_h)$ and $\hat{e}_\tau(\tilde{G}_{i,h}^{(\bar{x})})$ are the error-indicator functions corresponding to u_h and $\tilde{G}_{i,h}^{(\bar{x})}$, respectively,

$$\mathcal{M}_i^{(2)}(\bar{\boldsymbol{x}}) = \sum_{\substack{\tau \in T_h \\ \tau \subset \tilde{\omega}_h}} \eta_\tau(u_h)\ \eta_\tau(\tilde{G}_{i,h}^{(\bar{x})}) \tag{44}$$

$$\mathcal{M}_i^{(3)}(\bar{\boldsymbol{x}}) = \sqrt{\sum_{\substack{\tau \in T_h \\ \tau \subset \tilde{\omega}_h}} (\eta_\tau(u_h))^2}\ \sqrt{\sum_{\substack{\tau \in T_h \\ \tau \subset \tilde{\omega}_h}} (\eta_\tau(\tilde{G}_{i,h}^{(\bar{x})}))^2} \tag{45}$$

We then have

$$\Big|\frac{\partial V_2^{\tilde{\omega}_h}}{\partial x_i}(\bar{\boldsymbol{x}})\Big| \le \mathcal{M}_i^{(1)}(\bar{\boldsymbol{x}}) \le \mathcal{M}_i^{(2)}(\bar{\boldsymbol{x}}) \le \mathcal{M}_i^{(3)}(\bar{\boldsymbol{x}}) \tag{46}$$

We will define the pollution-indicators $\mu_\tau^{(m)}(\bar{\boldsymbol{x}})$, $m = 1, 2$, by

$$\mu_{i,\tau}^{(1)}(\bar{\boldsymbol{x}}) := \Big| B_\tau\Big(\hat{e}_\tau(u_h), \hat{e}_\tau(\tilde{G}_{i,h}^{(\bar{x})})\Big)\Big|, \quad \mu_{i,\tau}^{(2)} := \eta_\tau(u_h)\ \eta_\tau(\tilde{G}_{i,h}^{(\bar{x})}) \tag{47}$$

We then have $\mathcal{M}_i^{(m)}(\bar{\boldsymbol{x}}) = \sum_{\substack{\tau \in T_h \\ \tau \subset \tilde{\omega}_h}} \mu_{i,\tau}^{(m)}(\bar{\boldsymbol{x}})$ for $i = 1, 2$, $m = 1, 2$. We will also define pollution-estimates for $|\nabla V_2^{\tilde{\omega}_h}|(\bar{\boldsymbol{x}})$ in the form

$$\mathcal{M}^{(m)}(\bar{\boldsymbol{x}}) := \sqrt{(\mathcal{M}_1^{(m)}(\bar{\boldsymbol{x}}))^2 + (\mathcal{M}_2^{(m)}(\bar{\boldsymbol{x}}))^2}\,, \qquad m = 1,2,3 \tag{48}$$

Remark 3.2. Although the derivations are valid only for the case where the error-indicators are based on the ERp estimate we can expect that the above estimates give reliable answers if they are computed using indicators other than ERp-indicators (provided that these indicators are reliable modulo the pollution).

4 The quality of the a-posteriori estimates of the pollution-error

We will give sample results on the a-posteriori estimation of the pollution error. We employed the estimates $\mathcal{M}^{(1)}$, $\mathcal{M}^{(2)}$, $\mathcal{M}^{(3)}$ given in Section 3 in the following form:

$$\mathcal{M}_k^{(i)} = \mathcal{M}_{k,sing}^{(i)} + \mathcal{M}_{k,smooth}^{(i)} \tag{49}$$

By $\mathcal{M}_{k,sing}^{(i)}$ (resp. $\mathcal{M}_{k,smooth}^{(i)}$) we denote the contributions to $\mathcal{M}_k^{(i)}$ from the elements adjacent to the singularity (resp. the elements in the rest of the mesh). For the meshes of triangles (resp. meshes of squares) we computed $\mathcal{M}_{k,sing}^{(i)}$ from the first layer (resp. the first two layers) of elements around the singular point. In the results the $\mathcal{M}_{k,smooth}^{(i)}$-part was computed using one of the indicators given in Section 2 (e.g. ERpP$p+3$, ERpB, *ZZ*) while the $\mathcal{M}_{k,sing}^{(i)}$-part was computed either by employing an extraction method or by employing the same indicators used in the interior. We also computed estimates for $|\nabla V_2^{\tilde{\omega}_h}(\bar{\boldsymbol{x}})|$ by combining the estimates for the x_1- and x_2-components.

In the numerical results we also computed the "exact" value of $\dfrac{\partial V_2^{\tilde{\omega}_h}}{\partial x_i}(\bar{\boldsymbol{x}})$ by solving the residual equation (26) for $\dfrac{\partial V_1^{\tilde{\omega}_h}}{\partial x_i}(\bar{\boldsymbol{x}})$ using elements of degree $(p+2)$ and by letting (see also [1])

$$\frac{\partial V_2^{\tilde{\omega}_h}}{\partial x_i}(\bar{\boldsymbol{x}}) = \frac{\partial e_h}{\partial x_i}(\bar{\boldsymbol{x}}) - \frac{\partial V_1^{\tilde{\omega}_h}}{\partial x_i}(\bar{\boldsymbol{x}}) \tag{50}$$

We measured the quality of the estimators by computing the effectivity indices

$$\kappa_i^{(m)} = \frac{\mathcal{M}_i^{(m)}}{\left|\dfrac{\partial V_2^{\tilde{\omega}_h}}{\partial x_i}(\bar{\boldsymbol{x}})\right|}\,, \quad i = 1,2, \qquad \kappa^{(m)} := \frac{\mathcal{M}^{(m)}}{|\nabla V_2^{\tilde{\omega}_h}(\bar{\boldsymbol{x}})|} \tag{51}$$

for $m = 1, 2, 3$.

In Table 3 we give an example of how the quality of the estimates of the pollution is affected by the quality of the error-indicators near the singular point. We considered the L-shaped domain with $\alpha = \frac{1}{3}$ and computed the pollution estimates at $\bar{\boldsymbol{x}} = (0.5, 0.5)$ for the uniform mesh of triangles shown in Fig. 5a $\left(h = \frac{1}{16}\right)$ for linear and quadratic triangles. We computed the pollution-estimates by employing the error-indicators from the ERpB estimator. The results in Table 3 show overestimation by a factor of 1.9-2.5 by the $\mathcal{M}^{(1)}$ and $\mathcal{M}^{(2)}$ pollution-estimates. This is due to the fact that the error-indicators for the ERpB estimator overestimate the error in the key elements (see the results in Tables 1a, 1b).

In order to be able to evaluate the performance of the pollution-estimates in the ideal case (without the influence of the quality of the particular indicators near the singular point) we also computed the error-indicators in the key elements using the extraction method as outlined above. In Table 4a (resp. Table 4b) we give the results for linear and quadratic triangles for $\alpha = \frac{1}{4}$ for the mesh shown in Fig. 5a $\left(\text{resp. } \alpha = \frac{1}{3} \text{ for the mesh shown in Fig. 4a}\right)$. In Tables 5a (resp. Table 5b) we give the results for bilinear (resp. biquadratic) squares for $\alpha = \frac{1}{3}$ and in Table 5c we give the results for $\alpha = \frac{1}{4}$ and biquadratic squares. In the above computations for the meshes of triangles we let

$$\tilde{\omega}_h := (\bar{x}_1 - 3h,\ \bar{x}_1 + 3h) \times (\bar{x}_2 - 3h,\ \bar{x}_2 + 3h) \tag{52}$$

while for the meshes of squares we used

$$\tilde{\omega}_h := (\bar{x}_1 - 2h,\ \bar{x}_1 + 3h) \times (\bar{x}_2 - 2h,\ \bar{x}_2 + 3h) \tag{53}$$

We observe that the $\mathcal{M}^{(1)}$ and $\mathcal{M}^{(2)}$ estimates of the pollution have effectivity indices between 0.9-1.4.

We also computed the $\mathcal{M}^{(3)}$-estimates of the pollution for the cases given in Tables 5a, 5b and 5c. We obtained the following effectivity indices

$$\kappa_1^{(3)} = 4.76, \qquad \kappa_2^{(3)} = 4.83, \qquad \kappa^{(3)} = 4.81 \tag{54}$$

for the case in Table 5a,

$$\kappa_1^{(3)} = 5.68, \qquad \kappa_2^{(3)} = 4.80, \qquad \kappa^{(3)} = 5.32 \tag{55}$$

for the case in Table 5b, and

$$\kappa_1^{(3)} = 16.53, \qquad \kappa_2^{(3)} = 13.43, \qquad \kappa^{(3)} = 14.77 \tag{56}$$

for the case in Table 5c. From these results we see that the $\mathcal{M}^{(3)}$-estimate grossly overestimates the pollution-error and should not be used.

In the Remark 3.2 above we noted that the derivations of the estimates for the pollution are *valid only when the ERp error-indicators are used but nevertheless* they could be computed from other error indicators too provided that these indicators are robust modulo the pollution. In Table 3 we gave examples of pollution estimates based on the ERpB error-indicators. To illustrate further the point of Remark 3.2 we computed the $\mathcal{M}^{(2)}$-estimates for the case in Tables 5a, 5b and 5c using the ZZ error-indicators. We obtained the following effectivity indices

$$\kappa_1^{(2)} = 1.16, \qquad \kappa_2^{(2)} = 1.33, \qquad \kappa^{(2)} = 1.24 \tag{57}$$

for the case given in Table 5a,

$$\kappa_1^{(2)} = 2.27, \qquad \kappa_2^{(2)} = 2.35, \qquad \kappa^{(2)} = 2.31 \tag{58}$$

for the case given in Table 5b, and

$$\kappa_1^{(2)} = 1.78, \qquad \kappa_2^{(2)} = 1.68, \qquad \kappa^{(2)} = 1.72 \tag{59}$$

for the case given in Table 5c. As in the case of the ERpB-based pollution estimate we get *(reasonable) overestimation* of the error which is related to overestimation by the ZZ error-indicators in the key elements.

5 Adaptive control of the pollution-error

Let $t\%$ be a given tolerance and let us assume that the goal is to construct a mesh T_h, by employing regular subdivision of the elements of an initial mesh T_h^0, such that

$$|||V_2^{\tilde{\omega}_h}|||_{\omega_h} \leq t\% \, |||V_1^{\tilde{\omega}_h}|||_{\omega_h} \tag{60}$$

where $\omega_h \subseteq T_h^0$. The mesh T_h, which achieves local control of the pollution-error in ω_h according to (60) may be obtained using the following algorithm:

1. Let $T_h \equiv T_h^0$ and go to 3.
2. For each element $\tau \in T_h$ do:
   2.1. Compute μ_τ, $\tau \in T_h$, $\tau \not\subseteq \tilde{\omega}_h$
   2.2. If $\mu_\tau \geq \gamma \max_\tau \mu_\tau$, subdivide τ.
3. Compute the finite element solution on T_h and $\mathcal{E}_{\omega_h}$.

4. Check if

$$\mathcal{M}_{\omega_h} \leq t\% \, \mathcal{E}_{\omega_h} \tag{61}$$

If not, go to 2, otherwise stop.

Here μ_τ is the pollution-indicator for the element τ, $\mathcal{M}_{\omega_h}$ is an estimator for $|||V_2^{\tilde{\omega}_h}|||_{\omega_h}$, $\gamma \in (0,1)$ is a user-specified constant. The algorithm may be also modified so that step 3 is executed only after a certain number of refinement steps. In the examples below we let ω_h coincide with an element $\bar{\tau}$ and we employed the estimate

$$\mathcal{M}_{\bar{\tau}} = \sqrt{|\bar{\tau}|} \sqrt{\left(\mathcal{M}_1^{(1)}(\bar{\boldsymbol{x}})\right)^2 + \left(\mathcal{M}_2^{(1)}(\bar{\boldsymbol{x}})\right)^2} \tag{62}$$

and for the refinement we used the pollution-indicators

$$\mu_\tau = \sqrt{\left(\mu_{1,\tau}^{(1)}\right)^2 + \left(\mu_{2,\tau}^{(2)}\right)^2} \tag{63}$$

where $\bar{\boldsymbol{x}}$ is taken to coincide with a vertex of the element $\bar{\tau}$.

We employed the above algorithm with $t\% = 10\%$ for meshes of bilinear and biquadratic squares in the L-shaped domain $\left(\alpha = \frac{1}{3}\right)$ for $\omega_h \equiv \bar{\tau} = (0.5, 0.625)^2$ (the element shown shaded gray in Figs. 7a, 7b). We employed, as the initial mesh, a uniform mesh of squares with $h_0 = \frac{1}{2}$ in the second and third quadrants and elements of size $h_0 = \frac{1}{8}$ in $\tilde{\omega}_h = [0.25, 0.75]^2$. In Fig. 7a (resp. Fig. 7b) we show the final mesh of bilinear (resp. biquadratic) squares constructed by the algorithm for which we have $\frac{\mathcal{M}_{\bar{\tau}}}{\eta_\tau} = 9.57\% < 10\%$ $\left(\text{resp. } \frac{\mathcal{M}_{\bar{\tau}}}{\eta_{\bar{\tau}}} = 9.81\% < 10\%\right)$. In both cases we employed the $\mathcal{M}^{(1)}$-estimate of the pollution computed using the error-indicators obtained from the extraction method in the key elements and the ERpP$p+3$ error-indicators in the rest of the mesh. We also note that in the initial uniform mesh of bilinear (resp. biquadratic) squares we have $\frac{\eta_{\bar{\tau}}}{|||e_h|||_{\bar{\tau}}} = 0.035$ $\left(\text{resp. } \frac{\eta_{\bar{\tau}}}{|||e_h|||_{\bar{\tau}}} = 0.017\right)$ while in the final mesh $\frac{\eta_{\bar{\tau}}}{|||e_h|||_{\bar{\tau}}} = 0.994$ $\left(\text{resp. } \frac{\eta_{\bar{\tau}}}{|||e_h|||_{\bar{\tau}}} = 0.923\right)$. Thus by controlling the pollution-error to less than 10% the value of the indicator η_τ we get a very reliable local indicator.

We also considered the domain ABCDEFGH shown in Fig. 8 and exact solution

$$u(x,y) = r_C^{\alpha_C} \sin\left(\frac{2}{3}\vartheta_C\right) + r_E^{\alpha_E} \sin\left(\frac{1}{3}\vartheta_E\right) \tag{64}$$

where $r_C = \sqrt{(x_1 - (x_C)_1)^2 + (x_2 - (x_C)_2)^2}$, $\vartheta_C = \tan^{-1}\left(\frac{x_2 - (x_C)_2}{x_1 - (x_C)_1}\right)$ and similarly for r_E and ϑ_E, $\alpha_C = \frac{2}{3}$ and $\alpha_E = \frac{1}{3}$. We let $\bar{\tau}$ be the element shown shaded in Fig. 8 and we adapted the mesh to achieve $|||V_2^{\tilde{\omega}}|||_{\bar{\tau}} \leq 20\% |||V_1^{\tilde{\omega}_h}|||_{\bar{\tau}}$. By $\tilde{\omega}_h$ we mean the patch which includes $\bar{\tau}$ and two mesh-layers around it. We employed quadratic element ($p = 2$) and we based the estimate $\mathcal{M}_{\bar{\tau}}$ and the pollution-indicators μ_τ on the ERpB. In Figs. 8a and 8b we give the pollution-adaptive meshes (obtained used $\gamma = 0.8$) for two locations of the element $\bar{\tau}$, (shown shaded gray with a bullet at the centroid). In both the examples, $\tilde{\omega}_h$ is the patch which includes all the shaded elements and one layer of elements around them. In Fig. 8a we show the final grid for which we have $\frac{\mathcal{M}_{\bar{\tau}}}{\eta_{\bar{\tau}}} = 18.6\% < 20\%$. For this mesh $\frac{\eta_{\bar{\tau}}}{|||e_h|||_{\bar{\tau}}} = 0.92$ while in the initial mesh $\frac{\eta_{\bar{\tau}}}{|||e_h|||_{\bar{\tau}}} \approx 0$. In Fig. 8b, for the second location of the element τ, we show the final grid for which $\frac{\mathcal{M}_{\bar{\tau}}}{\eta_{\bar{\tau}}} = 29.8\% < 30\%$. For this mesh, $\frac{\eta_\tau}{|||e_h|||_\tau} \approx 0$. We also computed the effectivity-index for the pollution-estimate $\mathcal{M}_\tau$ for the final mesh shown in Fig. 8a; its value was found 1.89. Hence we note that the pollution-estimates were based on ERpB produce slight overrefinement of the mesh.

6 Summary of conclusions

In this work we constructed a-posteriori estimates for the pollution-error. The main tools are the local error-indicators and a finite-element approximation of the Green's function. We also proposed an algorithm for the adaptive control of the pollution-error in any patch of interest.

The major conclusions of this study are:

1. The quality of the estimates of the pollution-error depends on the quality of the error-indicators near the singular points. Existing estimators over- or underestimate the error in the key elements depending on the unsmoothness of the solution and the degree of the elements. Hence it is necessary to construct estimators with element effectivity indices close to one near the singular points. This will be addressed in another work.

2. It is possible to control the pollution-error in any patch of elements by refining the elements with the biggest pollution-indicators.

3. When a direct solver is used the cost of the pollution-estimates is negligible. It is practically the same cost as computing with a few additional right-hand sides.

4. For elements of degree $p \geq 2$ it is also possible to construct estimates of the pollution in the value of the finite element solution. This will be addressed in a future paper.

7 Acknowledgments

The work of I. B. was supported by the office of Naval Research under contract N00014-90-J-1030 and by the National Science Foundation under Grant CCR-88-20279. The work of T.S., C.S.U. and S.K.G. was supported by the U.S. Army Research Office under Grant DAAL03-G-028, by the National Science Foundation under Grant MSS-9025110 and by the Texas Advanced Research Program under Grant TARP-71071.

References

1. I. Babuška, T. Strouboulis, A. Mathur and C.S. Upadhyay, 'Pollution error in the h-version of the finite element method and the local quality of a-posteriori error estimators', *Technical Note BN-1163*, Institute for Physical Science and Technology, University of Maryland, College Park, February 1994.

2. I. Babuška, T. Strouboulis, C.S. Upadhyay and S.K. Gangaraj, 'Pollution error in the h-version of the finite element method and the local quality of recovered derivatives', in preparation.

3. I. Babuška, R. Durán and R. Rodriguez, 'Analysis of the efficiency of an a-posteriori error estimator for linear triangular finite elements', *SIAM J. Numer. Anal.* 29 (4), (1992) 947-964.

4. I. Babuška, L. Plank and R. Rodriguez, 'Quality assessment of the a-posteriori error estimation in finite elements', *Finite Elements in Analysis and Design*, 11 (1992) 285-306.

5. I. Babuška, L. Plank and R. Rodriguez, 'Basic problems of a-posteriori error estimation', *Comput. Methods Appl. Mech. Engrg.* 101 (1992) 97-112.

6. I. Babuška, T. Strouboulis and C.S. Upadhyay, 'A model study of the quality of a-posteriori estimators for linear elliptic problems: Error estimation in the interior of patchwise uniform grids of triangles', *Comput. Methods Appl. Mech. Engrg.* 114 (1994) 307-378.

7. I. Babuška, T. Strouboulis, C.S. Upadhyay, S.K. Gangaraj and K. Copps, 'Validation of a-posteriori error estimators by numerical approach', *Internat. J. Numer. Methods Engrg.* 37 (1994), 1073-1123.

8. I. Babuška, T. Strouboulis, C.S. Upadhyay and S.K. Gangaraj, 'A model study of element residual estimators for linear elliptic problems: The quality of the estimators in the interior of meshes of triangles and quadrilaterals', *Technical Note BN-1171*, Institute for Physical Science and Technology, University of Maryland, College Park, May 1994.

9. I. Babuška, T. Strouboulis, C.S. Upadhyay and S.K. Gangaraj, 'Study of superconvergence by a computer-based approach. Superconvergence of the gradient in finite element solutions of Laplace's and Poisson's equation', *Technical Note BN-1155*, Institute for Physical Science and Technology, University of Maryland, College Park, November 1993.

10. I. Babuška, T. Strouboulis and C.S. Upadhyay, 'η%-superconvergence of finite element approximations in the interior of general me-shes of triangles', *Technical Note BN-1160*, Institute for Physical Science and Technology, University of Maryland, College Park, December 1993.

11. I. Babuška, T. Strouboulis, S.K. Gangaraj and C.S. Upadhyay, 'η%-superconvergence in the interior of locally refined meshes of quadrilaterals. Superconvergence of the gradient in finite element solutions of Laplace's and Poisson's equations', *Technical Note BN-1161*, Institute for Physical Science and Technology, University of Maryland, College Park, January 1994.

12. I. Babuška, T. Strouboulis, C.S. Upadhyay and S.K. Gangaraj, 'Superconvergence of the gradient of the displacement, the strain and stress in finite element solutions for plane elasticity', *Technical Note BN-1164*, Institute for Physical Science and Technology, University of Maryland, College Park, February 1994.

13. I. Babuška, T. Strouboulis, S.K. Gangaraj and C.S. Upadhyay, 'Validation of recipes for the recovery of stresses and derivatives by a computer-based approach', *Technical Note BN-1170*, Institute for Physical Science and Technology, University of Maryland, College Park, May 1994.

14. J.B. Ransom and N.F. Knight Jr., 'Global/Local analysis for composite panels', *Computers & Structures*, 37 (1990) 375-395.

15. M.A. Aminpour, S.L. McCleary, J.B. Ransom and J.M. Housner, 'A global/ local analysis for treating details structural design, in Adaptive, Multilevel and Hierarchical Computational Strategies', A.K. Noor, ed. AMD-Vol. 157, *Amercian Society of Mechancical Engineers*, New York (1992) 119-137.

16. M.A. Aminpour, J.B. Ransom and S.L. McCleary, 'Coupled analysis of independently modeled finite element subdomains', in the *Proceedings of the 33rd AIAA Structures*, Structural Dynamics and Materials Conference, Part 1, Structures I', American Institute of Astronautics and Aeronautics (1992) 109-120.

17. J. Fish and S. Markolefas, 'Adaptive global-local refinement strategy based on the interior error estimates of the h-method', *Internat. J. Numer. Methods Engrg.* 37 (1994) 827-838.

18. O.C. Zienkiewicz and J.Z. Zhu, 'The superconvergent patch recovery and a posteriori error estimates. Part 1: The recovery technique', *Internat. J. Numer. Methods Engrg.* 33, (1992) 1331-1364.

19. O.C. Zienkiewicz and J.Z. Zhu, 'The superconvergent patch recovery and a posteriori error estimates. Part 2: Error estimates and adaptivity', *Internat. J. Numer. Methods Engrg.* 33 (1992) 1365-1382.

20. O.C. Zienkiewicz and J.Z. Zhu, 'The superconvergent patch recovery (SPR) and adaptive finite element refinement', *Comput. Methods Appl. Mech. Engrg.* 101 (1992) 207-224.

21. P. Ladeveze, Comparison de models de milieux continus, 'These de Doctorat d'Etat es Sciences Mathematiques', L'Université Paris VI, 1975.

22. P. Ladeveze, 'Nouvelle procedure d'estimation d'erreur relative a le methode des elements finis et applications', *Journées Elements Finis* (1977) Rennes.

23. P. Ladeveze and D. Leguillon, 'Error estimate procedure in the finite element method and applications', *SIAM J. Numer. Anal.* 20 (1983) 485-509.

24. R.E. Bank and A. Weiser, 'Some a posteriori error estimators for elliptic partial differential equations', *Math. Comp.* 44 (1985) 283-301.

25. P. Ladeveze, J.P. Pelle and P. Rougeot, 'Error estimation and mesh optimization for classical finite elements', *Engineering Computations* 9, (1991) 69-80.

26. P. Ladeveze, P. Marin, J.P. Pelle and G.L. Gastine, 'Accuracy and optimal meshes in finite element computation for nearly compressible material', *Comput. Methods Appl. Mech. Engrg.* 94, (1992) 303-315.

27. M. Ainsworth and J.T. Oden, 'A unified approach to a-posteriori error estimation using element residual methods', *Numer. Math.* 65 (1993) 23-50.

28. J.T. Oden, L. Demkowicz, W. Rachowicz and T.A. Westermann, 'Toward a universal h-p adaptive finite element strategy: Part 2, A Posteriori Error Estimates', *Comput. Methods Appl. Mech. Engrg.* 77 (1989) 113-180.

29. T.A. Westermann, 'A Posteriori Estimation of Errors in hp finite element methods for linear elliptic boundary value problems', M.Sc. Thesis, The University of Texas at Austin (1989).

30. B.A. Szabo and I. Babuška, 'Finite Element Analysis', John Wiley & Sons, Inc., New York, 1991.

31. V.A. Kondrat'ev, 'Boundary problems for elliptic equations in domains with conical or angular points', *Transactions of the Moscow Mathematical Society*, (1967) 227-313.

32. P. Grisvard, 'Elliptic problems in nonsmooth domain', (Pitman, London, 1985).

33. I. Babuška and B.Q. Guo, 'Regularity of the solution of elliptic problems with piecewise analytic data. Part I. Boundary value problems for linear elliptic equations of second order', *SIAM J. Math. Anal.* 19 (1) (1988) 172-203.

34. I. Babuška and B.Q. Guo, 'Regularity of the solution of elliptic problems with piecewise analytic data. Part II: The trace space and applications to the boundary value problems with non-homogeneous boundary conditions', *SIAM J. Math. Anal.* 20 (1989) 763-781.

35. L.B. Wahlbin, 'On the sharpness of certain local estimates for $\overset{0}{H}{}^1$ Projections into Finite Element Spaces: Influence of a reentrant corner', *Math. Comp.* 42 (1984) 1-8.

36. L.B. Wahlbin, 'Local behavior in finite element methods', in: P.G. Ciarlet and J.L. Lions, eds., Handbook of Numerical Analysis, Vol. II (North-Holland, Amsterdam, 1991) 357-522.

37. H. Blum and R. Rannacher, 'Extrapolation techniques for reducing the pollution effect of reentrant corners in the finite element method', *Numer. Math.* 52 (1988) 539-564.

Appendix

We will now outline the recipe for the local construction of equilibrated element-residuals which is employed in the numerical examples. This construction was proposed in [21]-[26]. We let θ^ε be a function defined piecewise as a q-degree polynomial on each edge ε. We define (see Fig. 2)

$$\theta^\varepsilon_{\tau_{out}} = \theta^\varepsilon \ , \quad \theta^\varepsilon_{\tau_{in}} = -\theta^\varepsilon \tag{A.1}$$

Given any interior element τ and q, $0 \leq q \leq p$, the aim is to determine edgewise q-degree polynomials θ^ε, such that

$$\mathcal{F}^{EQ}_\tau(v) = \mathcal{F}_\tau(v) + \sum_{\varepsilon \in \partial\tau} \int_\varepsilon \theta^\varepsilon_\tau v = 0 \qquad \forall\ v \in S^q_h(\tau) \tag{A.2}$$

The residuals which satisfy (A.2) are said to be *q-order equilibrated*. Eq. (A.2) is equivalent to

$$\sum_{\varepsilon \subseteq \partial\tau} \int_\varepsilon \theta^\varepsilon_\tau \phi_i = -\mathcal{F}_\tau(\phi_i) \ , \qquad i = 1, \ldots, N^q_\tau \tag{A.3}$$

where ϕ_i is the i-th shape-function of the element and N^q_τ denotes the dimension of $S^q_h(\tau)$.

A.1 Equilibration for an interior vertex X

A set of edgewise polynomial corrections for edges connected to interior vertices is constructed as follows:

a. Linear corrections.

Let us first determine edgewise linear corrections in the form

$$\theta^\varepsilon = (\theta^{\varepsilon,1}\psi^\varepsilon_1 + \vartheta^{\varepsilon,2}\psi^\varepsilon_2) \tag{A.4}$$

$$\psi^\varepsilon_1 := \frac{2}{|\varepsilon|}(2\lambda^\varepsilon_1 - \lambda^\varepsilon_2), \qquad \psi^\varepsilon_2 := \frac{2}{|\varepsilon|}(2\lambda^\varepsilon_2 - \lambda^\varepsilon_1) \tag{A.5}$$

where λ^ε_k, $k = 1, 2$ are the linear shape-functions defined over the edge ε. Note that

$$\theta^{\varepsilon,k} = \int_\varepsilon \theta^\varepsilon \lambda^\varepsilon_k \ , \qquad k = 1, 2 \tag{A.6}$$

Let X denote an interior vertex of the mesh with the element τ^X_i and the edges ε^X_i, $i = 1, \ldots, 4$, connected to it, as shown in Fig. 9a and let $\nu(\varepsilon^X_k)$ denote the local number (1 or 2) of the vertex X with respect to the edge ε^X_k. The values of $\theta^{\varepsilon^X_k, \nu(\varepsilon^X_k)}$ are obtained from the linear system

$$\sum_{\varepsilon \subseteq \partial \tau_k^X} \int_\varepsilon \theta^\varepsilon_{\tau_k^X} \phi_X = -\mathcal{F}_{\tau_k^X}(\phi_X) \,, \qquad k = 1, \ldots, 4 \tag{A.7}$$

which reads

$$\begin{bmatrix} 1 & 0 & 0 & -1 \\ -1 & 1 & 0 & 0 \\ 0 & -1 & 1 & 0 \\ 0 & 0 & -1 & 1 \end{bmatrix} \begin{Bmatrix} \theta^{\varepsilon_1^X, \nu(\varepsilon_1^X)} \\ \theta^{\varepsilon_2^X, \nu(\varepsilon_2^X)} \\ \theta^{\varepsilon_3^X, \nu(\varepsilon_3^X)} \\ \theta^{\varepsilon_4^X, \nu(\varepsilon_4^X)} \end{Bmatrix} = \begin{Bmatrix} -\mathcal{F}_{\tau_1^X}(\phi_X) \\ -\mathcal{F}_{\tau_2^X}(\phi_X) \\ -\mathcal{F}_{\tau_3^X}(\phi_X) \\ -\mathcal{F}_{\tau_4^X}(\phi_X) \end{Bmatrix} \tag{A.8}$$

Here we assumed that the directions of edge-normals are the ones shown in Fig. 9a.

The matrix has exactly one zero eigenvalue with corresponding eigenvector $[1,1,1,1]^T$. Moreover from the *orthogonality condition* we have

$$\sum_{k=1}^{4} \mathcal{F}_\tau(\phi_X) = 0 \tag{A.9}$$

and the system is consistent. Particular solutions can be obtained from various choices of the free-constant. For example one may choose $\theta^{\varepsilon_4^X, \nu(\varepsilon_4^X)} = 0$ (e.g. [24]) or one may choose the constant by minimizing various norms of the solution of (A.8), namely

$$J(\{\theta^{\varepsilon_k^X, \nu(\varepsilon_k^X)}\}_{k=1}^4) = \sum_{k=1}^{4} w_k (\theta^{\varepsilon_k^X, \nu(\varepsilon_k^X)})^2 \tag{A.10}$$

where w_k denotes the weight associated with ε_k^X. Here we employed the choice $w_k = \dfrac{1}{|\varepsilon_k^X|}$ (see [25]).

b. Higher-order corrections.

Let us denote by $\phi_{\varepsilon,k}$, $k = 1, \ldots, (q+1)$ the basis-functions which do not vanish on the edge ε. We extend the conjugate basis introduced in (A.5) as follows:

$$\int_\varepsilon \psi_i^\varepsilon \phi_{\varepsilon,j} = \begin{cases} 0, & \text{if } j < i \\ \\ 1, & \text{if } j = 1 \end{cases} \tag{A.11}$$

where $3 \leq i, j \leq (q+1)$. After the linear edge corrections have been determined, the higher-order corrections can be computed from

$$\theta^{\varepsilon,i} = -\mathcal{F}_{\tau_{out}}(\phi_{\varepsilon,i}) - \sum_{j=1}^{i-1} \theta^{\varepsilon,j} \int_\varepsilon \psi_j \phi_{\varepsilon,i} \,, \quad i = 3, \ldots, (q+1), \quad \varepsilon \subseteq \partial \tau_{out} \tag{A.12}$$

Note that the higher-order corrections can be determined explicitly and are defined uniquely for each edge.

A.2 Equilibration for a vertex X on the boundary of the domain.

The edgewise polynomial corrections for edges connected to boundary-nodes are constructed as follows:

a. Linear corrections.

Let X be a vertex on the boundary of the domain, with elements τ_i^X, $i = 1, \ldots, 3$ and edges ε_j^X, $j = 1, \ldots, 4$ connected to it, as shown in Fig. 9b. The edges ε_1^X and ε_4^X lie on the boundary. For the vertex X we get the following linear system

$$\sum_{\varepsilon \subseteq \partial \tau_k^X} \int_\varepsilon \theta^\varepsilon_{\tau_k^X} \phi_X = -\mathcal{F}_{\tau_k^X}(\phi_X), \qquad k = 1, 2, 3. \tag{A.13}$$

which reads as,

$$\begin{bmatrix} -1 & 1 & 0 & 0 \\ 0 & -1 & 1 & 0 \\ 0 & 0 & -1 & 1 \end{bmatrix} \begin{Bmatrix} \theta^{\varepsilon_1^X, \nu(\varepsilon_1^X)} \\ \theta^{\varepsilon_2^X, \nu(\varepsilon_2^X)} \\ \theta^{\varepsilon_3^X, \nu(\varepsilon_3^X)} \\ \theta^{\varepsilon_4^X, \nu(\varepsilon_4^X)} \end{Bmatrix} = \begin{Bmatrix} -\mathcal{F}_{\tau_1^X}(\phi_X) \\ -\mathcal{F}_{\tau_2^X}(\phi_X) \\ -\mathcal{F}_{\tau_3^X}(\phi_X) \end{Bmatrix} \tag{A.14}$$

The directions of the edge normals are shown in Fig. 9b. We will have various possibilities for the type of boundary conditions on edges ε_1^X and ε_4^X. Based on these possibilities a solution to the above system is obtained. The following types of boundary conditions are possible:

(i) *Dirichlet boundary conditions on both edges ε_1^X and ε_4^X:*

The system (A.14) has an infinite set of solutions. A particular solution which minimizes (A.10) is selected.

(ii) *Neumann boundary conditions on both edges ε_1^X and ε_4^X:*

The system (A.14) has a unique solution which is obtained by setting $\theta^{\varepsilon_1^X, \nu(\varepsilon_1^X)}$ and $\theta^{\varepsilon_4^X, \nu(\varepsilon_4^X)}$ equal to zero.

(iii) *One of the edges ε_1^X, ε_4^X is on the Dirichlet boundary while the other is on the Neumann boundary:*

A unique solution is obtained for the system (A.14) by setting $\theta^{\varepsilon_k^X, \nu(\varepsilon_k^X)}$ equal to zero for the edge on the Neumann boundary.

b. Higher-order corrections.

The higher-order corrections are computed following exactly the same steps as for the interior vertex.

List of Figures

Effectivity indices in the elements in the neighborhood of the singular point					
Uniform mesh of linear triangles ($p = 1$)					
Element No.	$\frac{\|\|\|e_h\|\|\|_\tau^2}{\|\|\|e_h\|\|\|_\Omega^2}$	$ERpPp+1$	$ERpB$	ZZ	$PRpPp+3$
$u(r,\vartheta) = r^{\frac{1}{3}} \sin(\frac{\vartheta}{3})$					
1	0.147	2.544	1.897	0.475	0.759
2	0.123	3.008	1.959	0.562	0.788
3	0.154	2.737	1.656	0.502	0.916
4	0.106	1.930	1.361	0.603	1.031
5	0.138	1.787	1.037	0.701	1.098
6	0.114	0.729	0.558	1.298	1.178
$u(r,\vartheta) = r^{\frac{2}{3}} \sin(\frac{2\vartheta}{3})$					
1	0.129	1.696	1.268	1.028	0.964
2	0.088	1.372	1.037	1.183	0.979
3	0.127	1.306	0.776	0.907	1.026
4	0.127	1.585	0.920	0.907	1.026
5	0.088	1.739	1.269	1.183	0.979
6	0.129	1.972	1.473	1.028	0.964

Table 1a. The quality of the error indicators in the neighborhood of the singular point: The element effectivity indices for the mesh and elements shown in Figs. 4a and 4b, respectively. Uniform mesh of linear triangles ($p = 1$), $h = \frac{1}{16}$, $u(r,\vartheta) = r^\alpha \sin(\alpha\vartheta)$ $\left(\alpha = \frac{1}{3}, \frac{2}{3}\right)$.

Effectivity indices in the elements in the neighborhood of the singular point					
Uniform mesh of linear triangles ($p = 1$)					
Element No.	$\frac{\|\|\|e_h\|\|\|_\tau^2}{\|\|\|e_h\|\|\|_\Omega^2}$	$ERpPp+1$	$ERpB$	ZZ	$PRpPp+3$
$u(r,\vartheta) = r^{\frac{1}{4}} \sin(\frac{\vartheta}{4})$					
1	0.111	2.861	2.133	0.300	0.575
2	0.099	3.498	2.250	0.461	0.608
3	0.190	2.071	1.667	0.565	0.774
4	0.108	2.625	1.575	0.561	0.943
5	0.079	1.718	1.231	0.868	1.086
6	0.172	1.076	0.687	1.009	1.143
$u(r,\vartheta) = r^{\frac{1}{2}} \sin(\frac{\vartheta}{2})$					
1	0.106	2.003	1.494	0.775	0.886
2	0.079	2.074	1.432	1.169	0.929
3	0.187	1.266	0.799	1.154	1.035
4	0.086	0.907	0.724	1.133	1.077
5	0.113	2.060	1.200	1.120	1.010
6	0.174	1.221	1.181	0.933	0.898

Table 1b. The quality of the error indicators in the neighborhood of the singular point: The element effectivity indices for the mesh and elements shown in Figs. 5a and 5b, respectively. Uniform mesh of linear triangles ($p = 1$), $h = \frac{1}{16}$, $u(r,\vartheta) = r^\alpha \sin(\alpha\vartheta)$ $\left(\alpha = \frac{1}{4}, \frac{1}{2}\right)$.

Effectivity indices in the elements in the neighborhood of the singular point					
Uniform mesh of quadratic triangles ($p = 2$)					
Element No.	$\frac{\|\|\|e_h\|\|\|_\tau^2}{\|\|\|e_h\|\|\|_\Omega^2}$	$ERpPp+1$	$ERpB$	ZZ	$PRpPp+3$
$u(r,\vartheta) = r^{\frac{1}{3}}\sin(\frac{\vartheta}{3})$					
1	0.164	2.370	1.915	0.513	0.593
2	0.155	2.655	2.153	0.574	0.657
3	0.163	2.397	1.914	0.572	0.779
4	0.147	1.776	1.441	0.662	0.898
5	0.155	1.407	1.086	0.848	0.986
6	0.146	0.681	0.493	1.266	1.046
$u(r,\vartheta) = r^{\frac{2}{3}}\sin(\frac{2\vartheta}{3})$					
1	0.170	1.543	1.275	1.178	0.833
2	0.148	1.361	1.084	1.256	0.939
3	0.171	1.002	0.713	1.079	1.037
4	0.171	1.201	0.881	1.079	1.037
5	0.148	1.650	1.325	1.256	0.939
6	0.170	1.791	1.474	1.178	0.833

Table 1c. The quality of the error indicators in the neighborhood of the singular point: The element effectivity indices for the mesh and the elements shown in Figs. 4a and 4b, respectively. Uniform mesh of quadratic elements ($p = 2$), $h = \frac{1}{16}$, $u(r,\vartheta) = r^\alpha \sin(\alpha\vartheta)$ $\left(\alpha = \frac{1}{3}, \frac{2}{3}\right)$.

Effectivity indices in the elements in the neighborhood of the singular point					
Uniform mesh of quadratic triangles ($p = 2$)					
Element No.	$\frac{\|\|\|e_h\|\|\|_\tau^2}{\|\|\|e_h\|\|\|_\Omega^2}$	$ERpPp+1$	$ERpB$	ZZ	$PRpPp+3$
$u(r,\vartheta) = r^{\frac{1}{4}} \sin(\frac{\vartheta}{4})$					
1	0.123	2.689	2.166	0.336	0.456
2	0.119	3.116	2.521	0.471	0.509
3	0.222	1.851	1.743	0.588	0.665
4	0.133	2.291	1.829	0.703	0.823
5	0.103	1.610	1.301	0.943	0.924
6	0.197	0.945	0.679	1.108	1.022
$u(r,\vartheta) = r^{\frac{1}{2}} \sin(\frac{\vartheta}{2})$					
1	0.125	1.820	1.485	1.895	0.732
2	0.114	1.824	1.471	1.192	0.828
3	0.234	1.130	0.798	1.263	1.009
4	0.117	0.866	0.640	1.313	1.046
5	0.128	1.698	1.326	1.289	0.957
6	0.232	1.044	1.019	0.981	0.775

Table 1d. The quality of the error indicators in the neighborhood of the singular point: The element effectivity indices for the mesh and the elements shown in Figs. 5a and 5b, respectively. Uniform mesh of quadratic elements ($p = 2$), $h = \frac{1}{16}$, $u(r,\vartheta) = r^\alpha \sin(\alpha\vartheta)$ $\left(\alpha = \frac{1}{4}, \frac{1}{2}\right)$.

Effectivity indices in the elements in the neighborhood of the singular point							
Uniform mesh of bilinear squares ($p = 1$)							
$u(r,\vartheta) = r^{\frac{1}{3}} \sin(\frac{\vartheta}{3})$							
Element No.	$\frac{\|\|\|e_h\|\|\|_\tau^2}{\|\|\|e_h\|\|\|_\Omega^2}$	ERpPp + 1	ERpPp + 2	ERpPp + 3	ERpPp + 4	PRpPp + 3	ZZ
1	0.005	0.667	0.709	0.796	0.807	0.811	0.408
2	0.008	0.325	0.471	0.487	0.509	0.510	0.403
3	0.008	0.821	0.864	0.923	0.933	0.892	0.686
4	0.005	0.527	0.538	0.557	0.559	0.600	0.477
5	0.006	1.240	1.358	1.443	1.468	1.219	1.107
6	0.287	0.770	0.859	0.990	1.012	1.106	0.795
7	0.313	0.798	0.845	1.008	1.020	1.014	0.727
8	0.009	2.389	2.456	2.904	2.922	2.716	0.627
9	0.007	0.883	1.057	1.110	1.141	1.207	0.887
10	0.262	1.084	1.212	1.402	1.434	1.381	1.555
11	0.006	0.757	0.816	0.938	0.954	0.974	0.347
12	0.006	1.284	1.457	1.540	1.574	1.613	2.379

Table 2. The quality of the error indicators in the neighborhood of the singular point: The element effectivity indices for the mesh and the elements shown in Fig. 6a and 6b, respectively. Uniform mesh of bilinear squares ($p = 1$), $h = \frac{1}{16}$, $u(r,\vartheta) = r^{\frac{1}{3}} \sin(\frac{\vartheta}{3})$.

A-posteriori estimates of the pollution-error					
Estimates based on the ERpB estimator					
Mesh-patch $\tilde{\omega}_h$ centered at $\bar{x} = (0.5, 0.5)$					
$u(r,\vartheta) = r^{\frac{1}{3}} \sin(\frac{\vartheta}{3})$					
Quantity v	Exact	$\mathcal{M}^{(1)}$		$\mathcal{M}^{(2)}$	
	v	$\tilde{v}$	$\kappa(\tilde{v})$	$\tilde{v}$	$\kappa(\tilde{v})$
Uniform mesh of linear triangles ($p = 1$)					
$\left\|\frac{\partial V_2^{\tilde{\omega}_h}}{\partial x_1}(\bar{x})\right\|$	.0332	.0631	1.90	.0640	1.92
$\left\|\frac{\partial V_2^{\tilde{\omega}_h}}{\partial x_2}(\bar{x})\right\|$	.0281	.0585	2.08	.0597	2.13
$\|\nabla V_2^{\tilde{\omega}_h}\|(\bar{x})$	.0435	.0860	1.98	.0875	2.01
Uniform mesh of linear triangles ($p = 2$)					
$\left\|\frac{\partial V_2^{\tilde{\omega}_h}}{\partial x_1}(\bar{x})\right\|$	.0157	.0382	2.43	.0382	2.43
$\left\|\frac{\partial V_2^{\tilde{\omega}_h}}{\partial x_2}(\bar{x})\right\|$	.0132	.0349	2.64	.0349	2.64
$\|\nabla V_2^{\tilde{\omega}_h}\|(\bar{x})$	.0205	.0517	2.52	.0517	2.52

Table 3. The quality of the a-posteriori estimates of the pollution-error: The exact values of $\left|\frac{\partial V_2^{\tilde{\omega}_h}}{\partial x_1}(\bar{x})\right|$, $\left|\frac{\partial V_2^{\tilde{\omega}_h}}{\partial x_2}(\bar{x})\right|$ or $|\nabla V_2^{\tilde{\omega}_h}|(\bar{x})$, the corresponding $\mathcal{M}^{(1)}$- and $\mathcal{M}^{(2)}$-estimates (computed by employing the error-indicators from the ERpB estimator) and the corresponding effectivity indices. Uniform mesh of linear ($p = 1$) or quadratic ($p = 2$) triangles shown in Fig. 4a $\left(h = \frac{1}{16}\right)$, $u(r,\vartheta) = r^{\frac{1}{3}} \sin(\frac{\vartheta}{3})$.

A-posteriori estimates of the pollution-error					
Estimates based on the extraction method					
Mesh-patch $\tilde{\omega}_h$ centered at $\bar{x} = (0.5, 0.5)$					
$u(r,\vartheta) = r^{\frac{1}{4}}\sin(\frac{\vartheta}{4})$					
Quantity v	Exact	$\mathcal{M}^{(1)}$		$\mathcal{M}^{(2)}$	
	v	$\tilde{v}$	$\kappa(\tilde{v})$	$\tilde{v}$	$\kappa(\tilde{v})$
Uniform mesh of linear triangles ($p = 1$)					
$\left\|\frac{\partial V_2^{\tilde{\omega}_h}}{\partial x_1}(\bar{x})\right\|$	.0498	.0459	0.92	.0527	1.05
$\left\|\frac{\partial V_2^{\tilde{\omega}_h}}{\partial x_2}(\bar{x})\right\|$	.0437	.0441	1.01	.0481	1.10
$\|\nabla V_2^{\tilde{\omega}_h}\|(\bar{x})$	.0663	.0637	0.96	.0714	1.08
Uniform mesh of quadratic triangles ($p = 2$)					
$\left\|\frac{\partial V_2^{\tilde{\omega}_h}}{\partial x_1}(\bar{x})\right\|$	.0293	.0276	0.94	.0307	1.05
$\left\|\frac{\partial V_2^{\tilde{\omega}_h}}{\partial x_2}(\bar{x})\right\|$	.0258	.0252	0.98	.0265	1.03
$\|\nabla V_2^{\tilde{\omega}_h}\|(\bar{x})$	.0390	.0374	0.96	.0406	1.04

Table 4a. The quality of the a-posteriori estimates of the pollution-error: The exact values of $\left|\frac{\partial V_2^{\tilde{\omega}_h}}{\partial x_1}(\bar{x})\right|$, $\left|\frac{\partial V_2^{\tilde{\omega}_h}}{\partial x_2}(\bar{x})\right|$ or $|\nabla V_2^{\tilde{\omega}_h}|(\bar{x})$, the corresponding $\mathcal{M}^{(1)}$- and $\mathcal{M}^{(2)}$-estimates (computed by employing the error-indicators from the extraction method in the key elements) and the corresponding effectivity indices. Uniform mesh of triangles shown in Fig. 5a, $h = \frac{1}{16}$, $u(r,\vartheta) = r^{\frac{1}{4}}\sin(\frac{\vartheta}{4})$. The error-indicators computed from the extraction method were employed in one mesh-layer around the singular point; the error-indicators from ERpP$p+3$ were employed in the rest of the mesh.

A-posteriori estimates of the pollution-error					
Estimates based on the extraction method					
Mesh-patch $\tilde{\omega}_h$ centered at $\bar{x} = (0.5, 0.5)$					
$u(r,\vartheta) = r^{\frac{1}{3}} \sin(\frac{\vartheta}{3})$					
Quantity v	Exact	$\mathcal{M}^{(1)}$		$\mathcal{M}^{(2)}$	
	v	$\tilde{v}$	$\kappa(\tilde{v})$	$\tilde{v}$	$\kappa(\tilde{v})$
Uniform mesh of linear triangles ($p = 1$)					
$\left\|\frac{\partial V_2^{\tilde{\omega}_h}}{\partial x_1}(\bar{x})\right\|$	.0332	.0343	1.03	.0382	1.15
$\left\|\frac{\partial V_2^{\tilde{\omega}_h}}{\partial x_2}(\bar{x})\right\|$	.0281	.0338	1.18	.0379	1.35
$\|\nabla V_2^{\tilde{\omega}_h}\|(\bar{x})$	.0435	.0482	1.11	.0538	1.24
Uniform mesh of quadratic triangles ($p = 2$)					
$\left\|\frac{\partial V_2^{\tilde{\omega}_h}}{\partial x_1}(\bar{x})\right\|$	.0157	.0152	0.97	.0161	1.03
$\left\|\frac{\partial V_2^{\tilde{\omega}_h}}{\partial x_2}(\bar{x})\right\|$	.0132	.0149	1.13	.0149	1.13
$\|\nabla V_2^{\tilde{\omega}_h}\|(\bar{x})$	.0205	.0209	1.02	.0219	1.07

Table 4b. The quality of the a-posteriori estimates of the pollution-error: The exact values of $\left|\frac{\partial V_2^{\tilde{\omega}_h}}{\partial x_1}(\bar{x})\right|$, $\left|\frac{\partial V_2^{\tilde{\omega}_h}}{\partial x_2}(\bar{x})\right|$ or $|\nabla V_2^{\tilde{\omega}_h}|(\bar{x})$ and the corresponding $\mathcal{M}^{(1)}$- and $\mathcal{M}^{(2)}$-estimates (computed by employing the error-indicators from the extraction method in the key elements) and the corresponding effectivity indices. Uniform mesh of triangles shown in Fig. 4a, $h = \frac{1}{16}$, $u(r,\vartheta) = r^{\frac{1}{3}} \sin(\frac{\vartheta}{3})$. The error-indicators computed from the extraction method were employed in one mesh-layer around the singular point; the error-indicators from ERpP$p+3$ were employed in the rest of the mesh.

A-posteriori estimates of the pollution-error					
Estimates based on the extraction method					
Uniform mesh of bilinear squares ($p = 1$)					
$u(r, \vartheta) = r^{\frac{1}{3}} \sin(\frac{\vartheta}{3})$					
Mesh-patch $\tilde{\omega}_h$ **centered at** $\bar{x} = (0.5, 0.5)$					
Quantity v_1	Exact	$\mathcal{M}^{(1)}(v_1)$		$\mathcal{M}^{(2)}(v_1)$	
	v	v_1	$\kappa(v_1)$	v_1	$\kappa(v_1)$
$\left\|\frac{\partial V_2^{\tilde{\omega}_h}}{\partial x_1}(\bar{x})\right\|$	0.0212	0.0242	1.14	0.0301	1.41
$\left\|\frac{\partial V_2^{\tilde{\omega}_h}}{\partial x_2}(\bar{x})\right\|$	0.0188	0.0199	1.06	0.0228	1.21
$\|\nabla V_2^{\tilde{\omega}_h}\|(\bar{x})$	0.0288	0.0314	1.09	0.0378	1.31

Table 5a. The quality of the a-posteriori estimates of the pollution-error: The exact values of $\left|\frac{\partial V_2^{\tilde{\omega}_h}}{\partial x_1}(\bar{x})\right|$, $\left|\frac{\partial V_2^{\tilde{\omega}_h}}{\partial x_2}(\bar{x})\right|$ or $|\nabla V_2^{\tilde{\omega}_h}|(\bar{x})$, the corresponding $\mathcal{M}^{(1)}$- and $\mathcal{M}^{(2)}$-estimates (computed by employing the error-indicators from the extraction method in the key elements) and the corresponding effectivity indices. Uniform mesh of bilinear squares ($p = 1$), $h = \frac{1}{16}$; $u(r, \vartheta) = r^{\frac{1}{3}} \sin(\frac{\vartheta}{3})$. The error-indicators computed from the extraction method were employed in two mesh-layers around the singular point; the error-indicators from ERpP$p + 3$ were employed in the rest of the mesh.

A-posteriori estimates of the pollution-error					
Estimates based on the extraction method					
Uniform mesh of biquadratic squares ($p = 2$)					
$u(r,\vartheta) = r^{\frac{1}{3}}\sin(\frac{\vartheta}{3})$					
Mesh-patch $\tilde{\omega}_h$ **centered at** $\bar{x} = (0.5, 0.5)$					
Quantity v_1	Exact	$\mathcal{M}^{(1)}(v_1)$		$\mathcal{M}^{(2)}(v_1)$	
	v	v_1	$\kappa(v_1)$	v_1	$\kappa(v_1)$
$\left\|\frac{\partial V_2^{\tilde{\omega}_h}}{\partial x_1}(\bar{x})\right\|$	0.0168	0.0202	1.20	0.0233	1.38
$\left\|\frac{\partial V_2^{\tilde{\omega}_h}}{\partial x_2}(\bar{x})\right\|$	0.0154	0.0177	1.15	0.0184	1.19
$\|\nabla V_2^{\tilde{\omega}_h}\|(\bar{x})$	0.0228	0.0269	1.18	0.0297	1.30

Table 5b. The quality of the a-posteriori estimates of the pollution-error: The exact values of $\left|\frac{\partial V_2^{\tilde{\omega}_h}}{\partial x_1}(\bar{x})\right|$, $\left|\frac{\partial V_2^{\tilde{\omega}_h}}{\partial x_2}(\bar{x})\right|$ or $|\nabla V_2^{\tilde{\omega}_h}|(\bar{x})$, the corresponding $\mathcal{M}^{(1)}$- and $\mathcal{M}^{(2)}$-estimates (computed by employing the error-indicators from the extraction method in the key elements) and the corresponding effectivity indices. Uniform mesh of biquadratic squares ($p = 2$), $h = \frac{1}{8}$; $u(r,\vartheta) = r^{\frac{1}{3}}\sin(\frac{\vartheta}{3})$. The error-indicators computed from the extraction method were employed in two mesh-layers around the singular point; the error-indicators from ERpP$p+3$ were employed in the rest of the mesh.

A-posteriori estimates of the pollution-error					
Estimates based on the extraction method					
Uniform mesh of biquadratic squares ($p = 2$)					
$u(r, \vartheta) = r^{\frac{1}{4}} \sin(\frac{\vartheta}{4})$					
Mesh-patch $\tilde{\omega}_h$ **centered at** $\bar{x} = (0.5, 0.5)$					
Quantity v_1	Exact	$\mathcal{M}^{(1)}(v_1)$		$\mathcal{M}^{(2)}(v_1)$	
	v	v_1	$\kappa(v_1)$	v_1	$\kappa(v_1)$
$\left\|\frac{\partial V_2^{\tilde{\omega}_h}}{\partial x_1}(\bar{x})\right\|$	0.0272	0.0332	1.22	0.0429	1.58
$\left\|\frac{\partial V_2^{\tilde{\omega}_h}}{\partial x_2}(\bar{x})\right\|$	0.0323	0.0397	1.23	0.0485	1.51
$\|\nabla V_2^{\tilde{\omega}_h}\|(\bar{x})$	0.0420	0.0517	1.23	0.0647	1.54

Table 5c. The quality of the a-posteriori estimates of the pollution-error: The exact values of $\left|\frac{\partial V_2^{\tilde{\omega}_h}}{\partial x_1}(\bar{x})\right|$, $\left|\frac{\partial V_2^{\tilde{\omega}_h}}{\partial x_2}(\bar{x})\right|$ or $|\nabla V_2^{\tilde{\omega}_h}|(\bar{x})$, the corresponding $\mathcal{M}^{(1)}$- and $\mathcal{M}^{(2)}$-estimates (computed by employing the error-indicators from the extraction method in the key elements) and the corresponding effectivity indices. Uniform mesh of bilinear squares ($p = 2$), $h = \frac{1}{8}$; $u(r, \vartheta) = r^{\frac{1}{4}} \sin(\frac{\vartheta}{4})$. The error-indicators computed from the extraction method were employed in two mesh-layers around the singular point; the error-indicators from ERpP$p + 3$ were employed in the rest of the mesh.

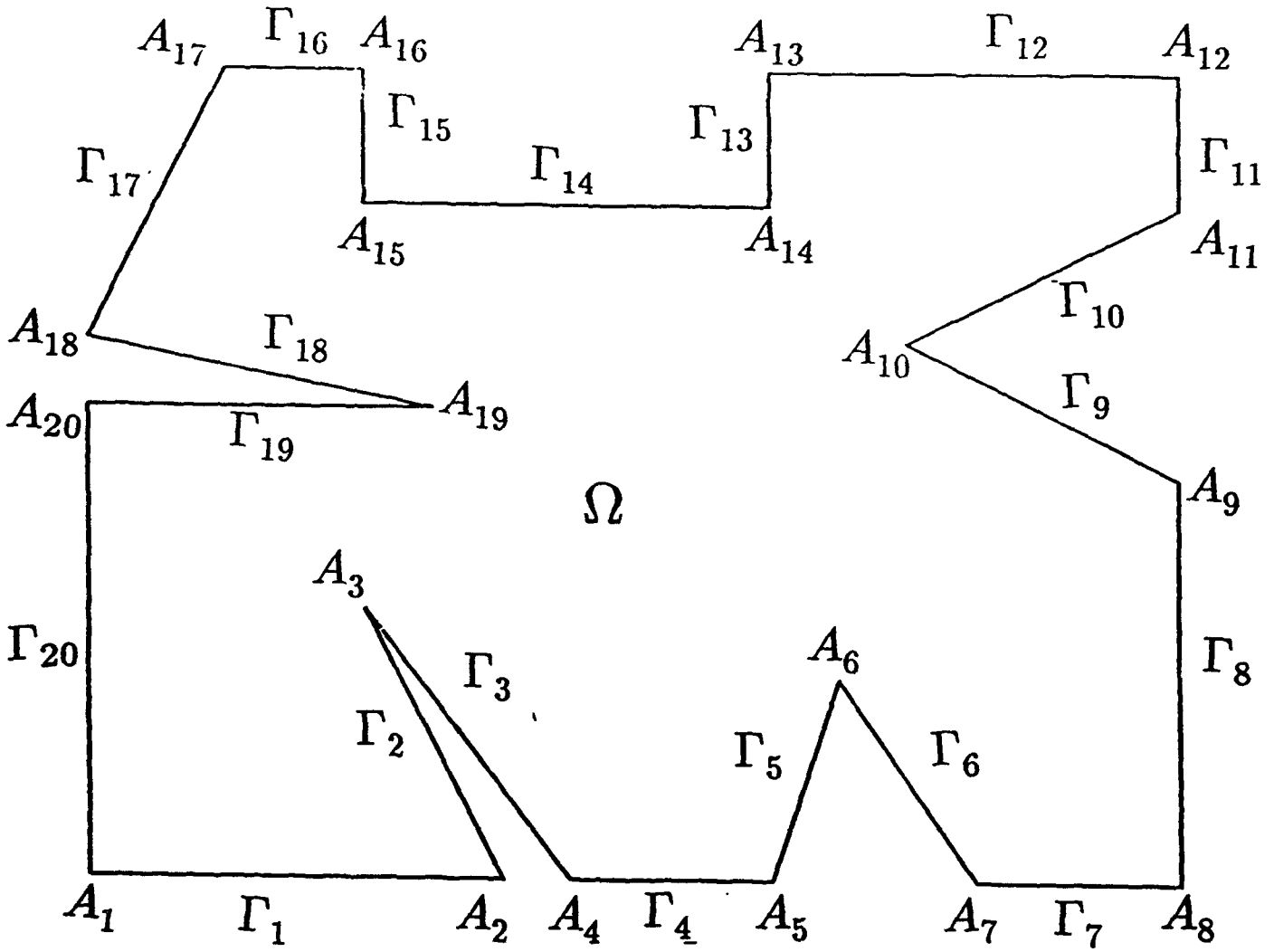
A_{17}
Γ_{16}
A_{16}
A_{13}
Γ_{12}
A_{12}
Γ_{15}
Γ_{13}
Γ_{17}
Γ_{14}
Γ_{11}
A_{15}
A_{14}
A_{11}
Γ_{10}
A_{18}
Γ_{18}
A_{10}
Γ_9
A_{20}
A_{19}
Γ_{19}
A_9
Ω
A_3
Γ_{20}
Γ_3
A_6
Γ_8
Γ_2
Γ_5
Γ_6
A_1
Γ_1
A_2
A_4
Γ_4
A_5
A_7
Γ_7
A_8

Fig. 1

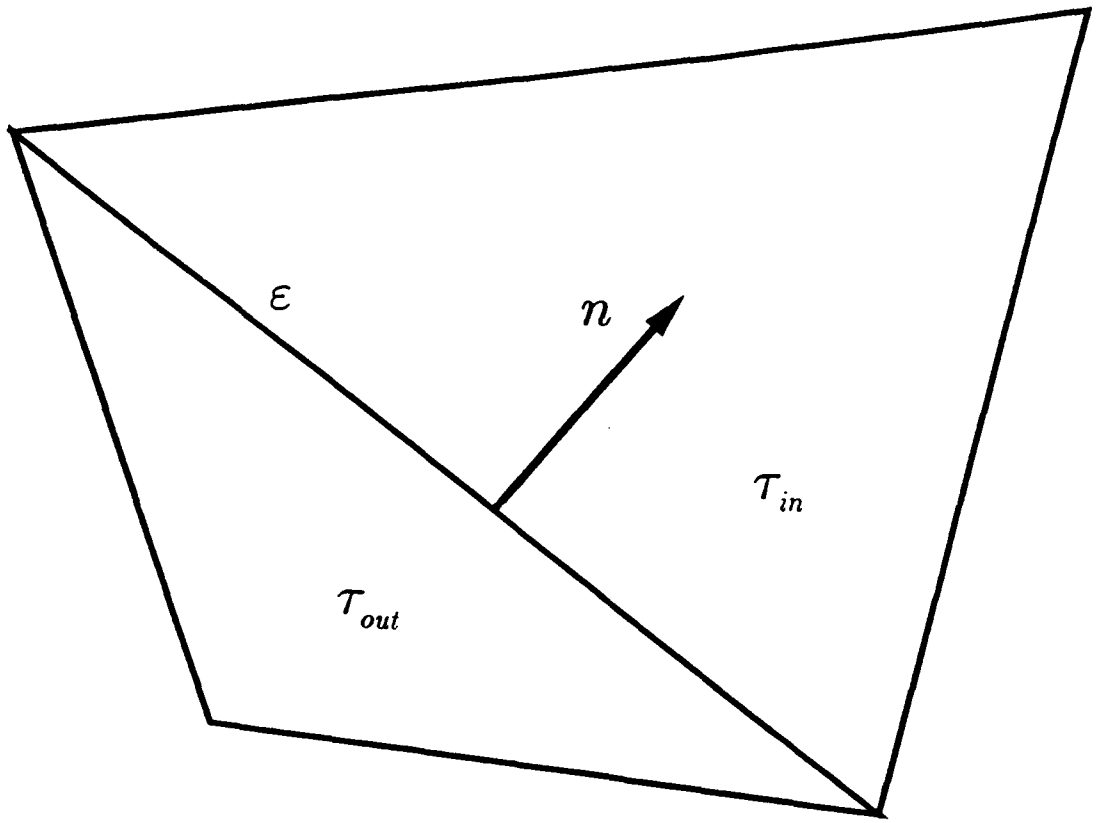

Fig. 2

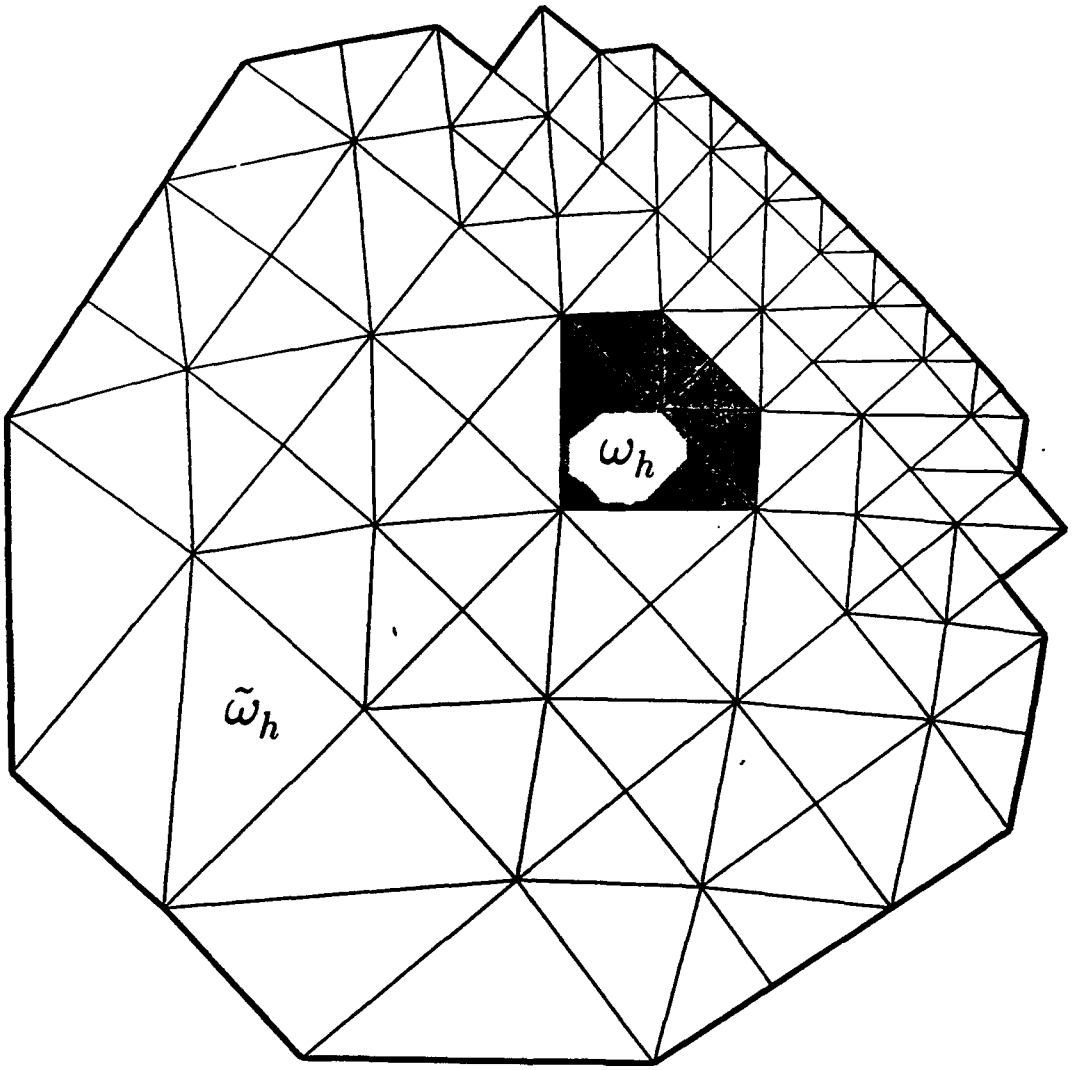

Fig. 3

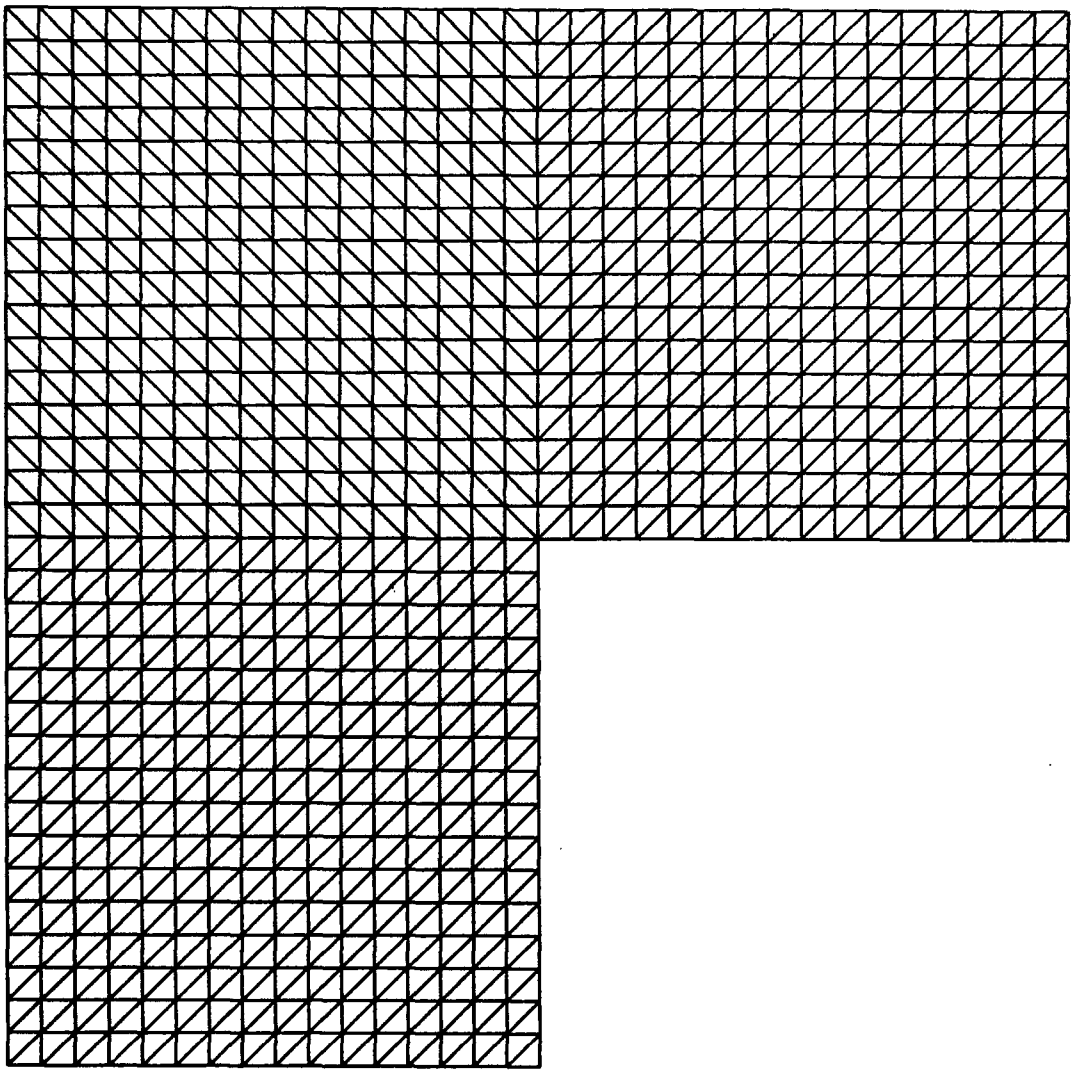

Fig. 4a

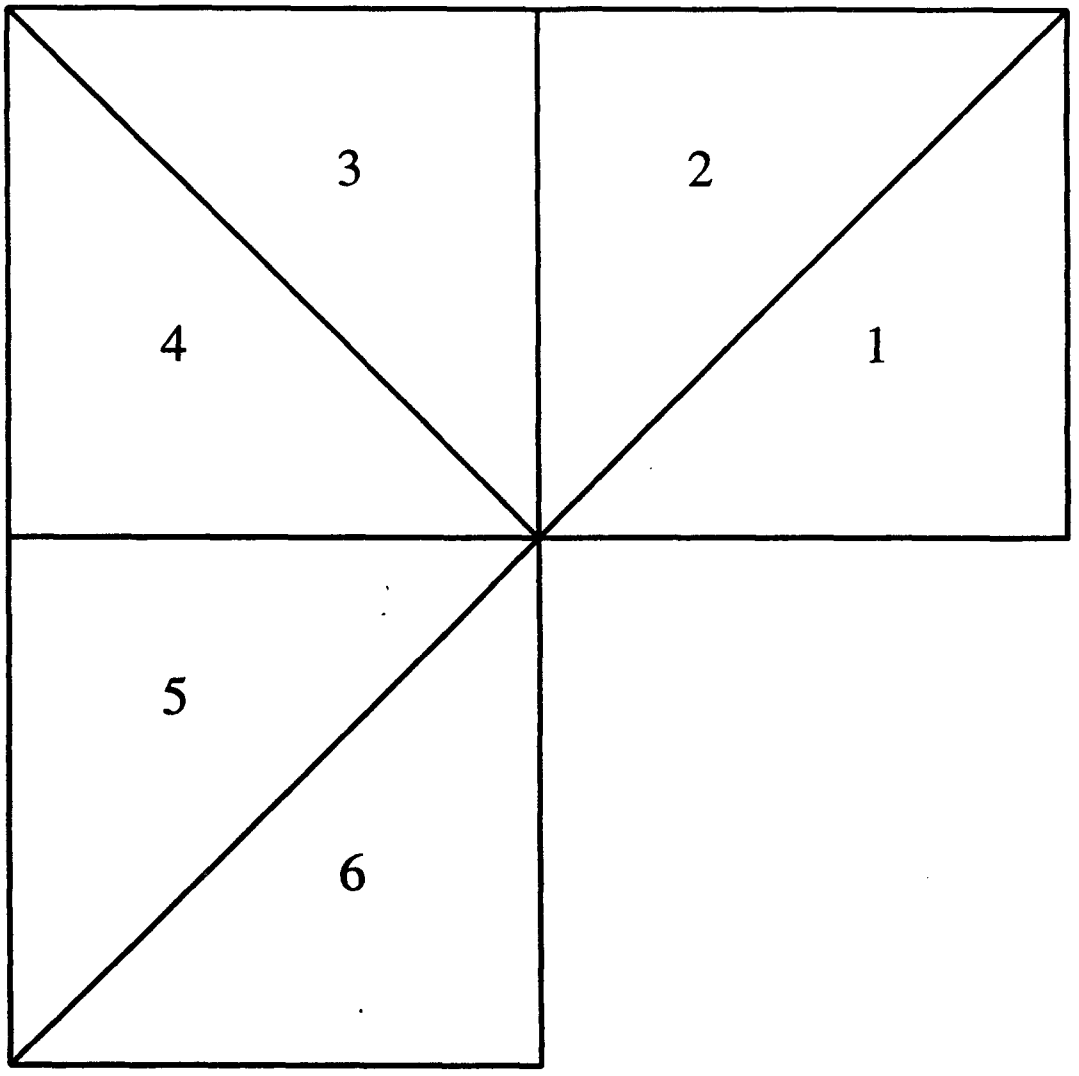

Fig. 4b

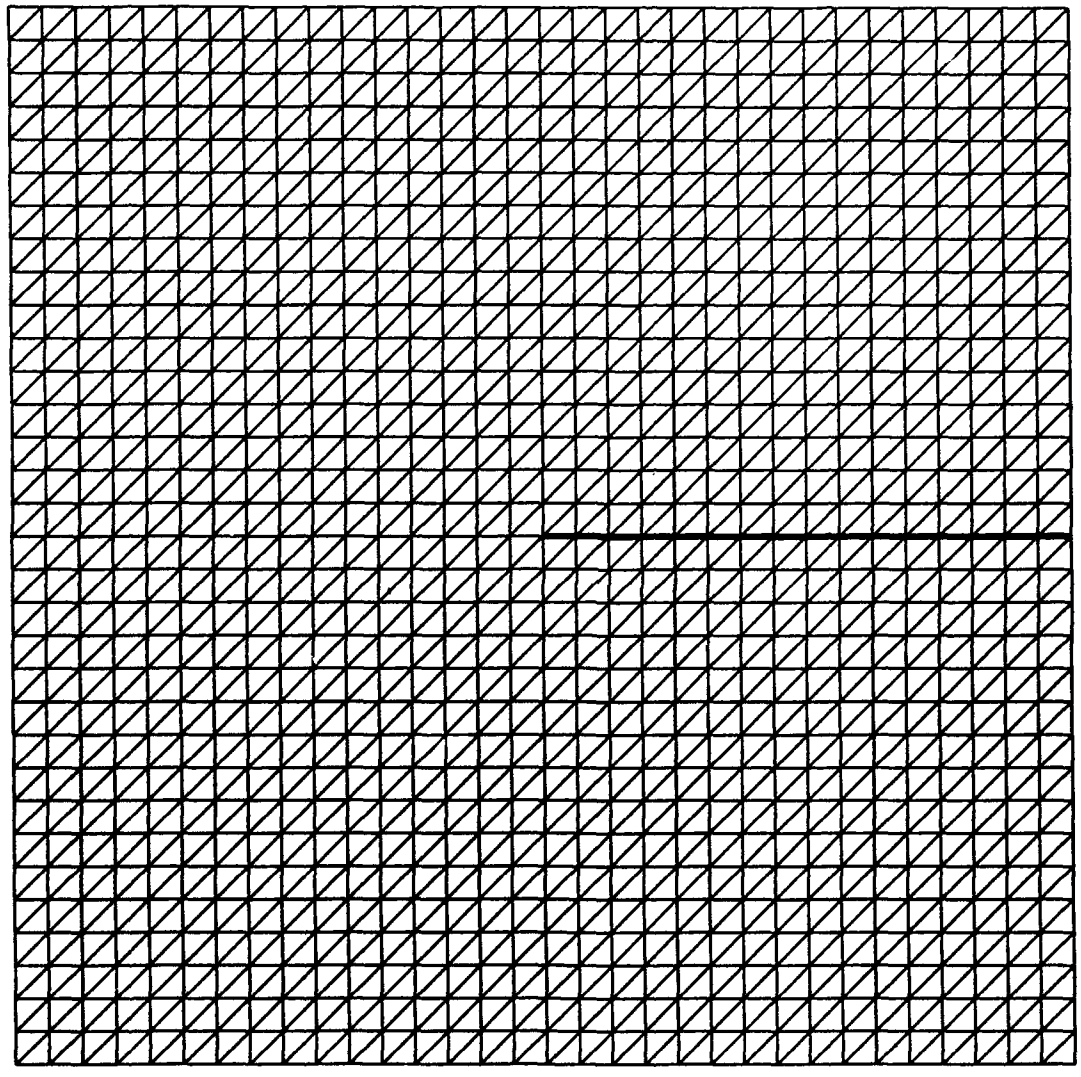

Fig. 5a

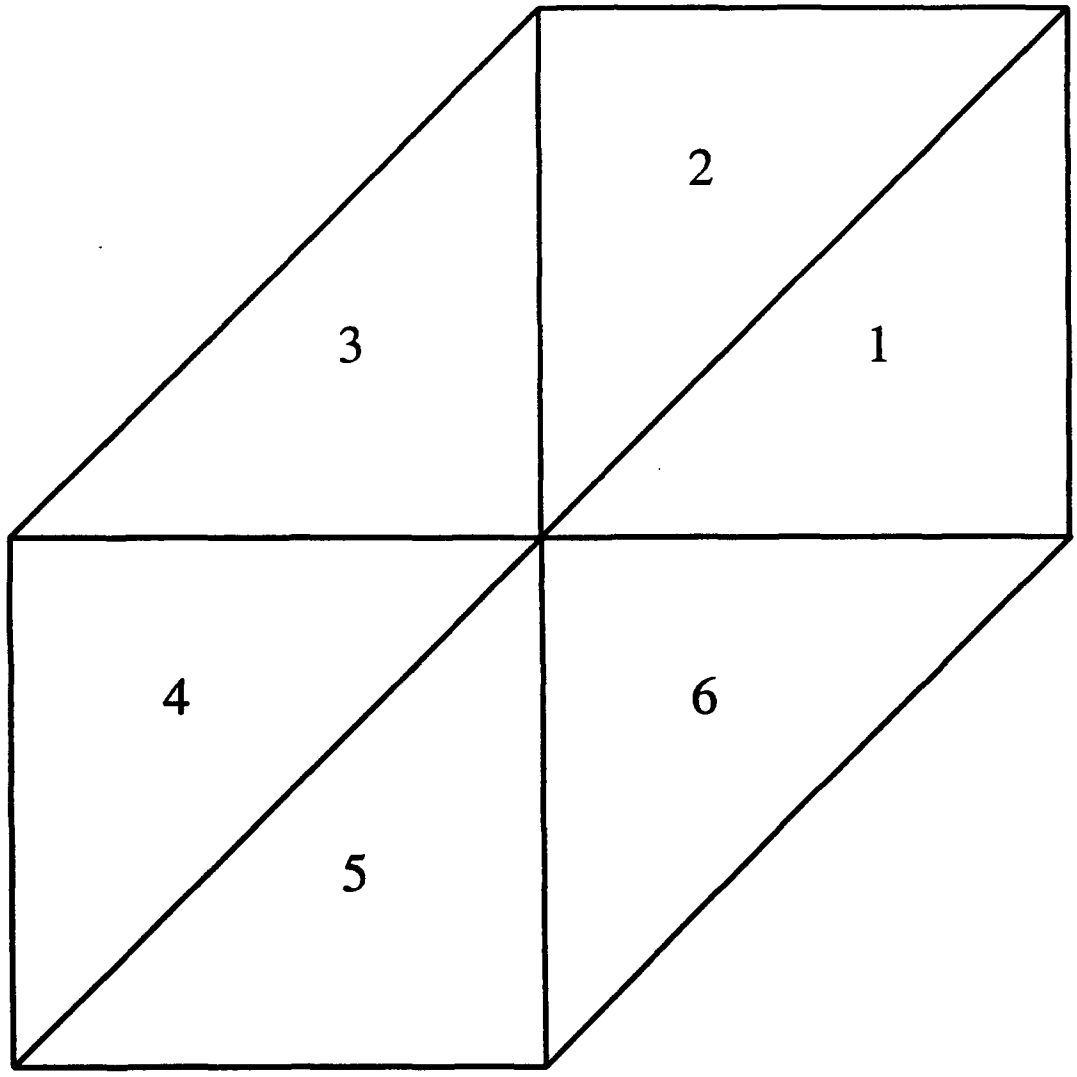

Fig. 5b

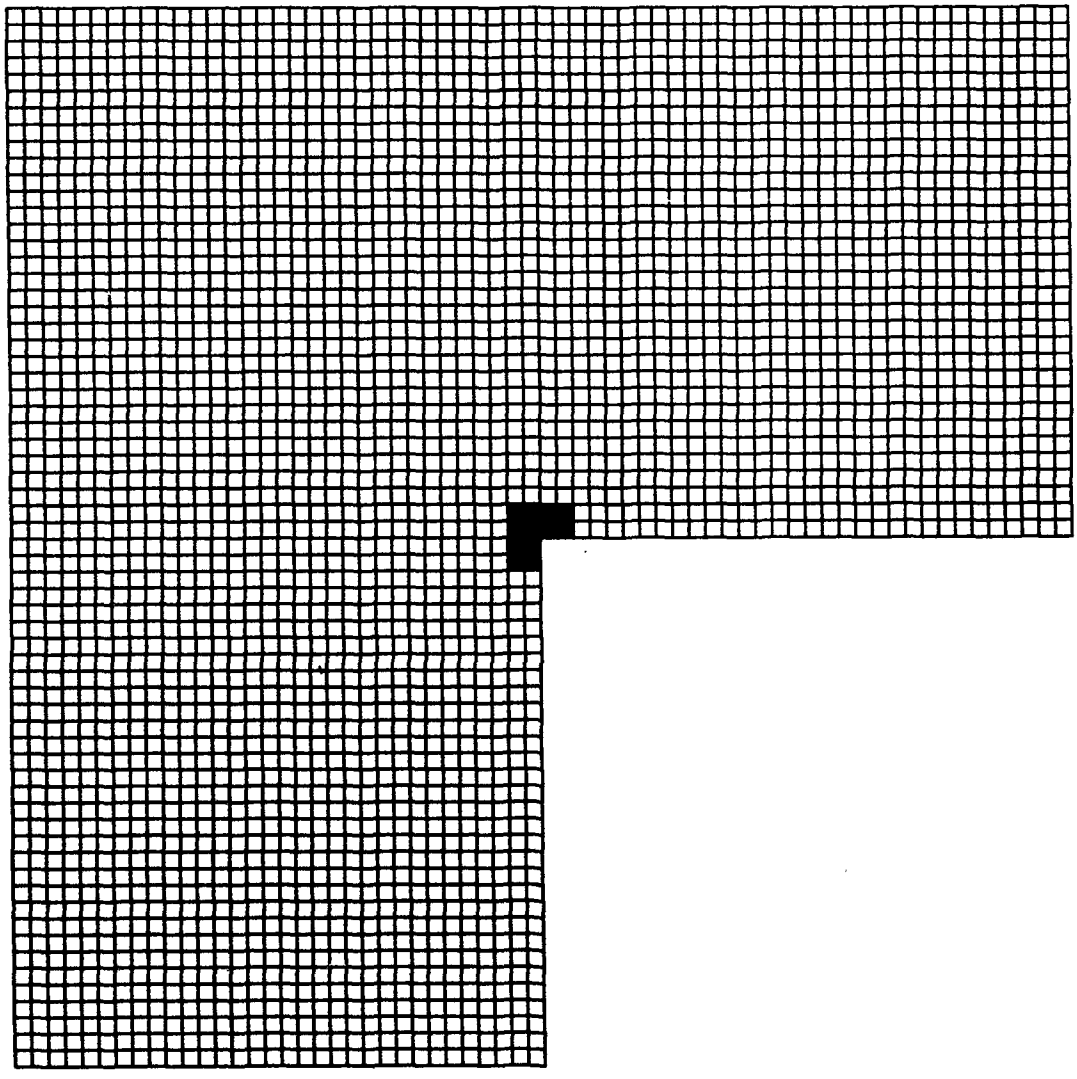

Fig. 6a

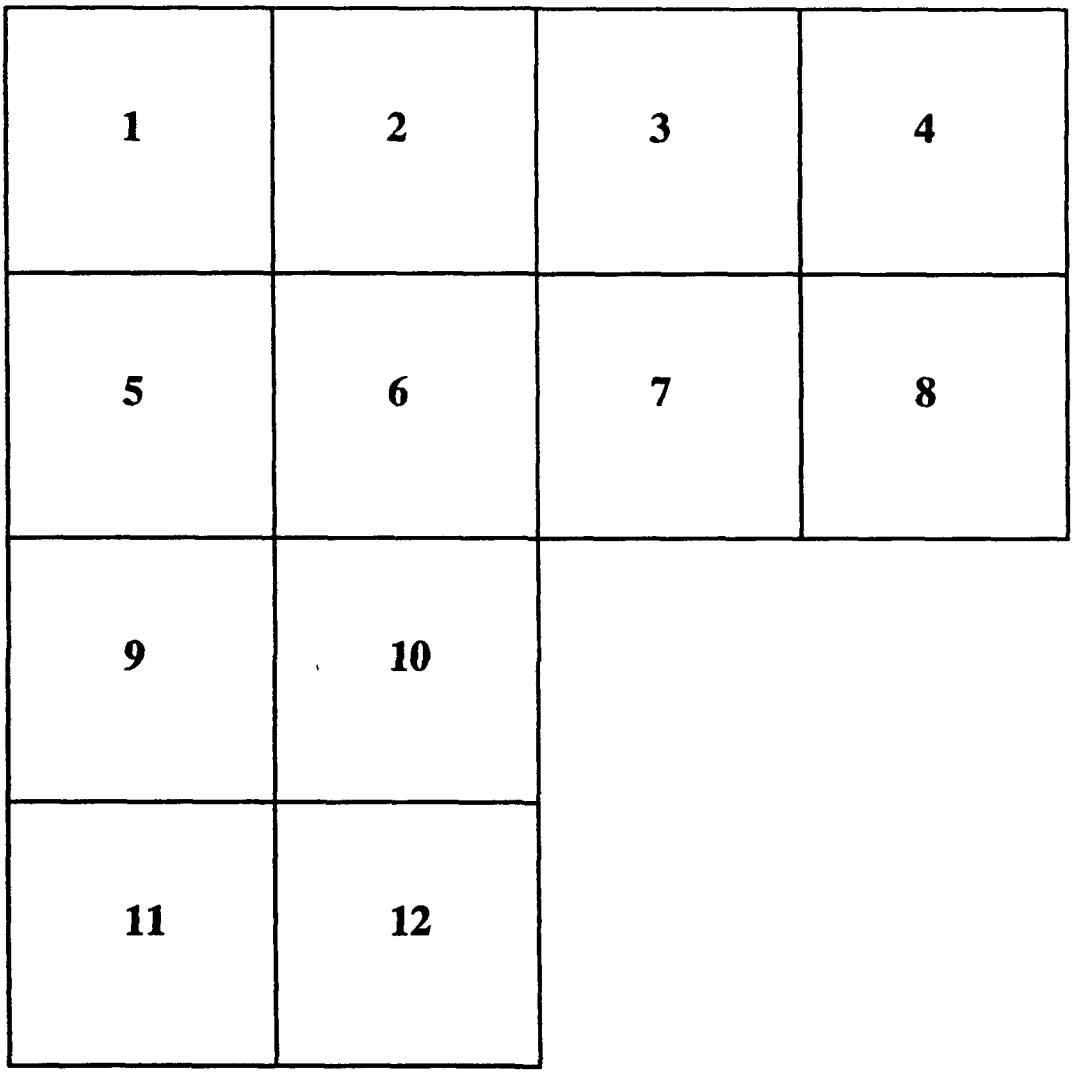

Fig. 6b

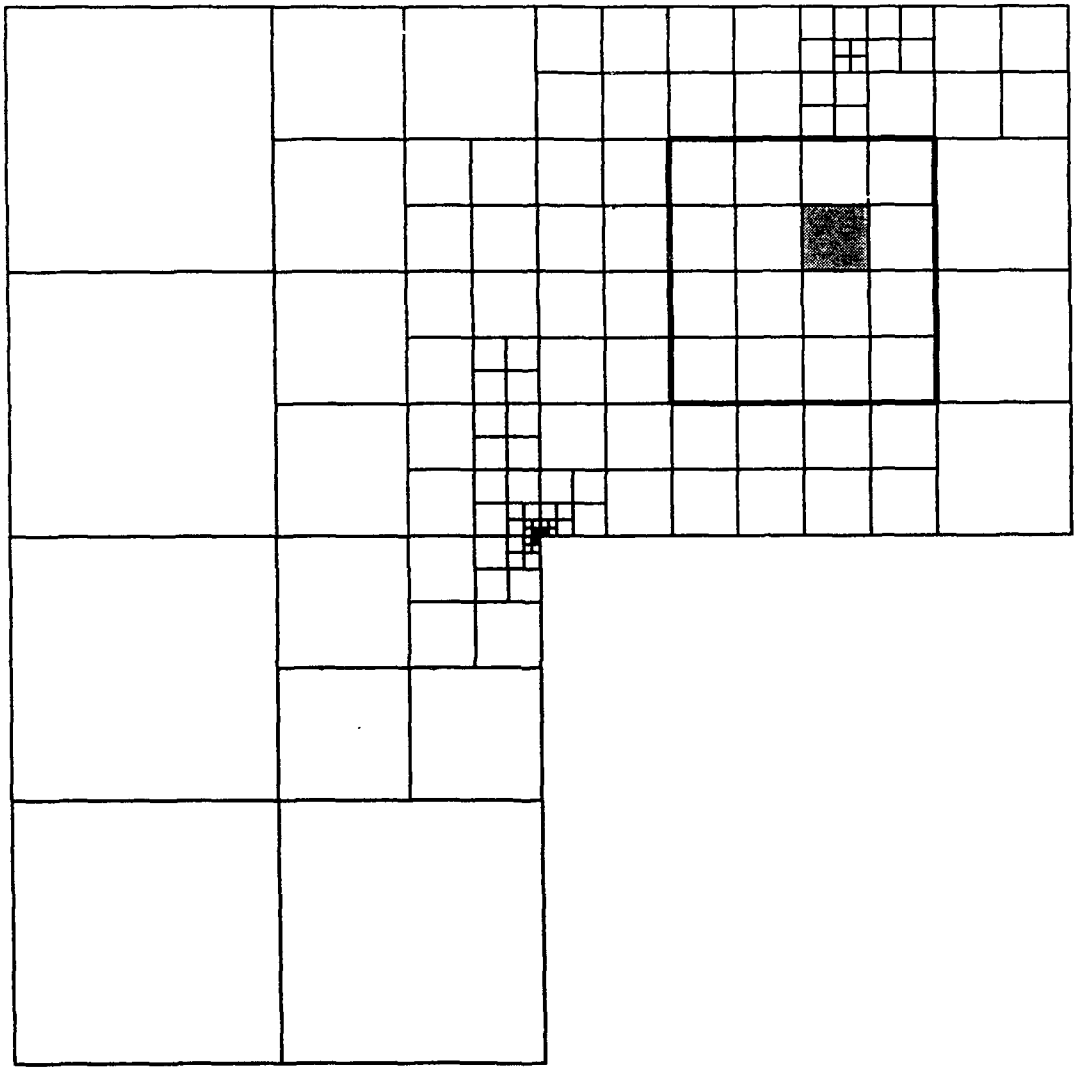

Fig. 7a

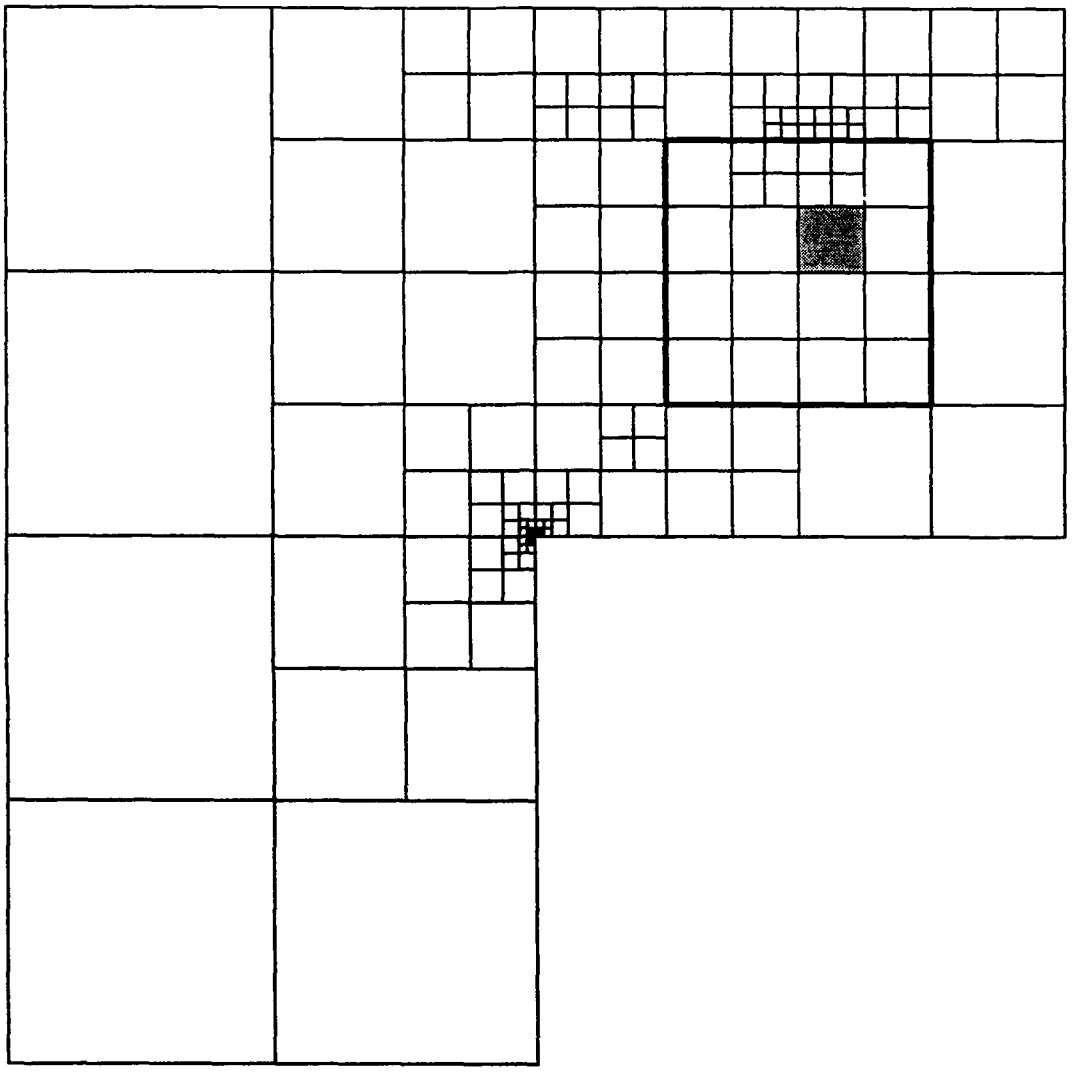

Fig. 7b

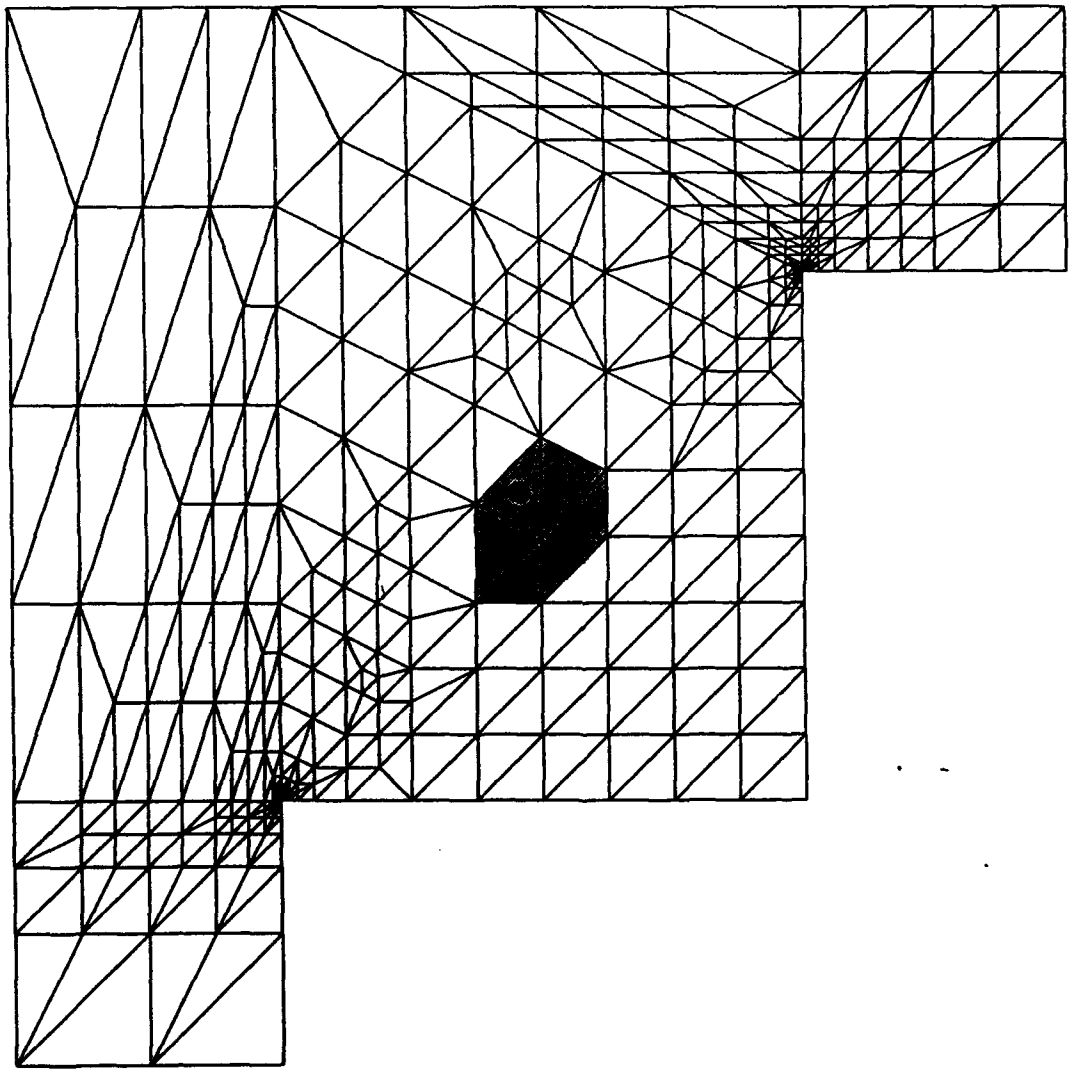

Fig. 8a

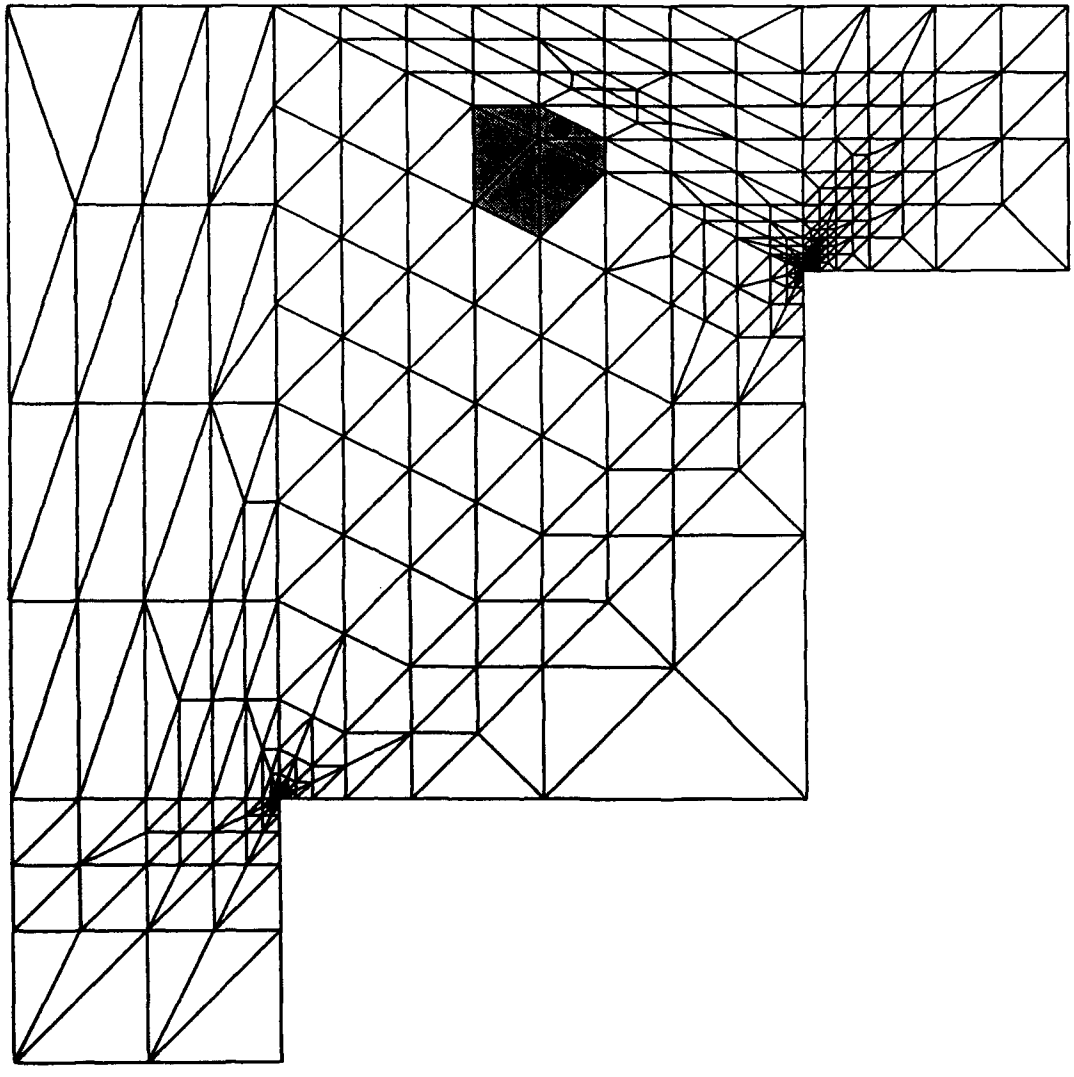

Fig. 8b

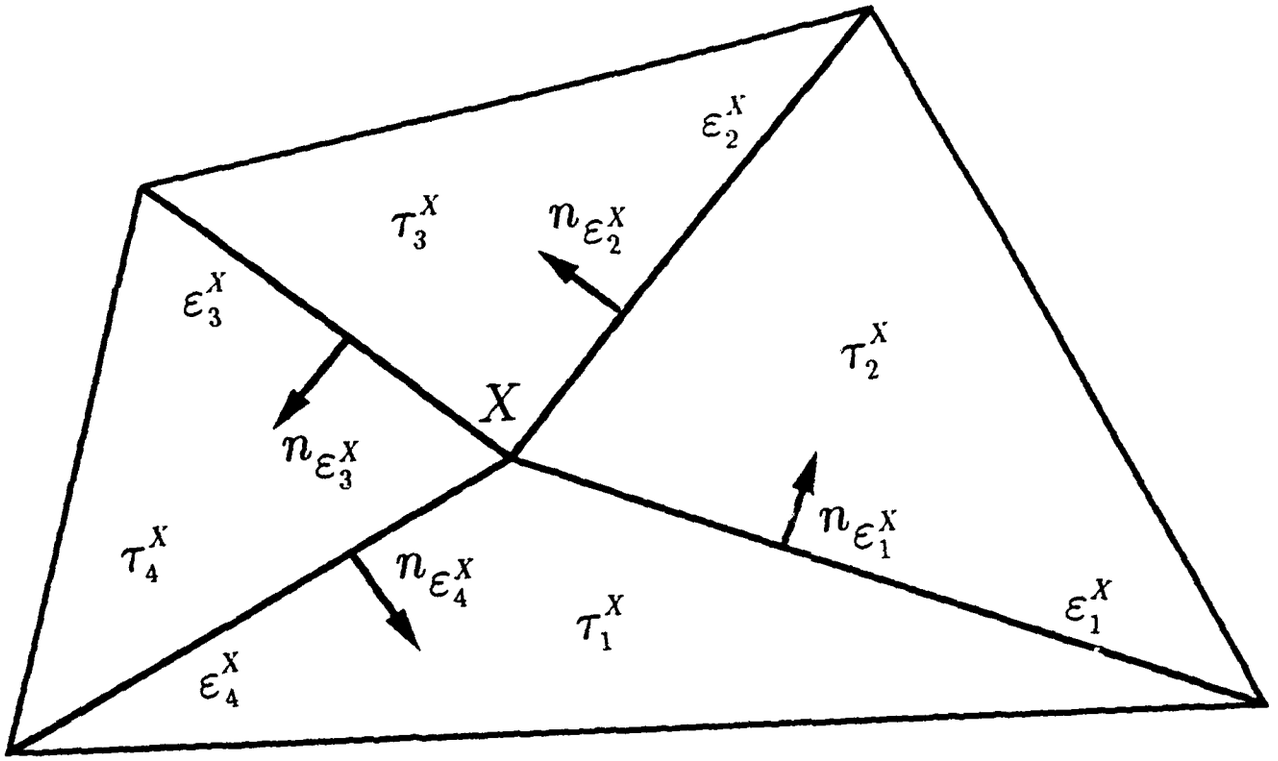
ε_2^X
τ_3^X
$n_{\varepsilon_2^X}$
ε_3^X
τ_2^X
X
$n_{\varepsilon_3^X}$
$n_{\varepsilon_1^X}$
τ_4^X
$n_{\varepsilon_4^X}$
ε_1^X
τ_1^X
ε_4^X

Fig. 9a

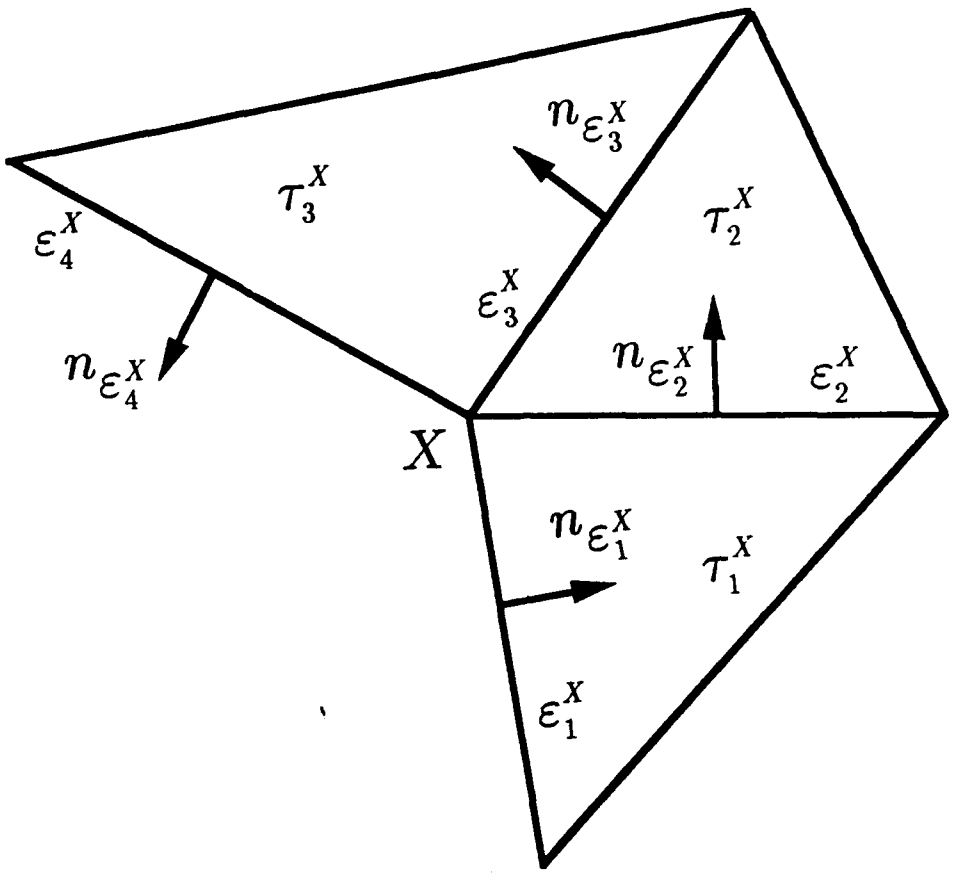
$n_{\varepsilon_3^X}$
τ_3^X
τ_2^X
ε_4^X
ε_3^X
$n_{\varepsilon_4^X}$
$n_{\varepsilon_2^X}$
ε_2^X
X
$n_{\varepsilon_1^X}$
τ_1^X
ε_1^X

Fig. 9b

The Laboratory for Numerical Analysis is an integral part of the Institute for Physical Science and Technology of the University of Maryland, under the general administration of the Director, Institute for Physical Science and Technology. It has the following goals:

To conduct research in the mathematical theory and computational implementation of numerical analysis and related topics, with emphasis on the numerical treatment of linear and nonlinear differential equations and problems in linear and nonlinear algebra.

To help bridge gaps between computational directions in engineering, physics, etc., and those in the mathematical community.

To provide a limited consulting service in all areas of numerical mathematics to the University as a whole, and also to government agencies and industries in the State of Maryland and the Washington Metropolitan area.

To assist with the education of numerical analysts, especially at the postdoctoral level, in conjunction with the Interdisciplinary Applied Mathematics Program and the programs of the Mathematics and Computer Science Departments. This includes active collaboration with government agencies such as the National Institute of Standards and Technology.

To be an international center of study and research for foreign students in numerical mathematics who are supported by foreign governments or exchange agencies (Fulbright, etc.).

Further information may be obtained from **Professor I. Babuška**, Chairman, Laboratory for Numerical Analysis, Institute for Physical Science and Technology, University of Maryland, College Park, Maryland 20742-2431.